SURFACE MODELLING

USING A

CLOSED UNIFORM BICUBIC B-SPLINE FORMULATION

by

Michael J. Van der Tol

A thesis
presented to the University of Manitoba
in partial fulfillment of the
requirements for the degree of
MASTER OF SCIENCE
in
ELECTRICAL ENGINEERING

Winnipeg, Manitoba, 1983

SURFACE MODELLING

USING A

CLOSED UNIFORM BICUBIC B-SPLINE FORMULATION

by

Michael J. Van der Tol

A thesis submitted to the Faculty of Graduate Studies of
the University of Manitoba in partial fulfillment of the requirements
of the degree of

MASTER OF SCIENCE

ABSTRACT

A surface modelling technique which implements a uniform bicubic B-spline formulation to interpolate closed and quasi-closed networks of points is presented. The formulation has the ability to model closed and quasi-closed surfaces while ensuring positional, first derivative, and second derivative continuity everywhere upon the surface. The surface continuity is achieved by transforming the control vertex structure to a closed form. As a consequence, explicit boundary derivative specification is avoided.

ACKNOWLEDGEMENTS

The author thanks Dr. A. Wexler for his supervision, guidance, and enthusiastic encouragement during the development of this work.

The author also wishes to thank his colleagues of the Numerical Applications Group at the University of Manitoba, for their constructive feedback related to this thesis topic.

Finally, the author thanks his wife, Cynthia, whose encouragement and support aided in the completion of this thesis.

CONTENTS

LIST OF PRINCIPAL SYMBOLS

$B_i(u)$	B-spline basis function on the parametric domain (u)
$B_j(v)$	B-spline basis function on the parametric domain (v)
$B_{i,j}(u,v)$	B-spline basis function on the two-dimensional parametric domain (uv)
$b_r(u)$	subsectional basis function on the unit parametric domain (u)
$b_s(v)$	subsectional basis function on the unit parametric domain (v)
[C]	control vertex coefficient matrix
i	generic index
j	generic index
k	generic index
m	number of curve segments in the parametric u-direction or number of surfaces patches in the parametric u-direction
n	number of surface patches in the parametric v-direction
$\underline{p}_i$	curve interpolation points in R^2 or R^3
$\underline{p}_{i,j}$	surface interpolation points in R^3
$[\underline{p}]$	vector of interpolation points
$\underline{P}(u,v)$	uniform bicubic B-spline surface
$\underline{P}_{i,j}(u,v)$	uniform bicubic B-spline surface patch
R^n	n-dimensional Euclidean space
S	set of all cubic splines

$\underline{S}(u)$	uniform cubic B-spline curve
$\underline{S}_i(u)$	uniform cubic B-spline curve segment
u	parametric variable
v	parametric variable
$\underline{V}_i$	curve control vertex in R^2 or R^3
$\underline{V}_{i,j}$	surface control vertex in R^3
$[\underline{V}]$	control vertex vector
$X(u)$	x-coordinate curve function
$Y(u)$	y-coordinate curve function
$Z(u)$	z-coordinate curve function

LIST OF FIGURES

LIST OF TABLES

Chapter I

INTRODUCTION

An increasingly popular method of delineating arbitrary three-dimensional objects has been the implementation of interpolating B-spline curves and surfaces. Early work by Coons[1] introduced the idea of representing surfaces by a collection of interconnected patches. However, the Coons patch formulation, in addition to requiring position and tangent information at patch corners, requires twist information in terms of corner 'cross-derivatives'. The specification of twist information usually requires the ability to visualize the interconnection between patches. Thus, it is commonplace to simply take the twist vector values as zero [2, 3]. This causes 'pseudoflats' or 'thumb-prints' in the surface representation [4, 5, 6].

More recently, Barsky [7, 6] has advocated the use of bicubic B-splines as open surface interpolants because of their ease of specification. The method provides up to second derivative continuity between adjoining surface patches without the specification of interpatch derivative information. To 'clamp down' the borders of the entire surface, and hence completely specify an open interpolating structure, Barsky's method requires positional, first

derivative, or second derivative boundary conditions. This led to the formation of symmetric, positive-definite, tridiagonal matrices and subsequently, fast, efficient solution algorithms to determine the controlling vertex structure.

Barsky did not address the problem of describing closed bicubic B-spline surfaces, which characteristically generate nonsymmetric, positive-definite, sparse matrices and are not readily solved.

Catmull and Clark [8] investigated the problem of describing closed surfaces by recursively subdividing B-spline surface patches over arbitrary meshes. Although the method is visually successful, there is no guarantee of derivative continuity at all mesh points.

A novel approach to modelling continuous closed and quasi-closed surfaces using a closed uniform bicubic B-spline formulation is presented in this thesis. Positional, first derivative, and second derivative continuity is ensured without explicit boundary derivative specification.

Based on a tensor product formulation, a rectangular vertex control mesh is transformed to a closed representation. This control mesh, when used in conjunction with the uniform bicubic B-spline basis, interpolates a prescribed closed or quasi-closed network of points. Positional, first derivative, and second derivative

continuity is enforced by incorporating control vertex constraint equations and patch-corner equations into a large system of linear equations.

The large system matrix is characteristically nonsymmetric and very sparse in nature. As a result, a modified bi-factorization method (after Zollenkopf [9]) is used to determine the locations of the control vertices.

Chapter II presents an introduction to cubic B-splines. Included is the derivation of the uniform cubic B-spline basis and the application of the cubic B-splines to curve interpolation.

Chapter III contains a presentation of the closed bicubic surface formulation. Included is a detailed discussion on the crucial aspects of surface continuity between merged patch boundaries. Quasi-closed bicubic surfaces, an extension of the closed formulation, are addressed to illustrate the flexibility in catering to other surface forms.

Closed and quasi-closed examples are covered in Chapter IV, demonstrating the algorithmic surface modelling package.

Chapter II

PARAMETRIC UNIFORM CUBIC B-SPLINE CURVES

2.1 SPLINES AND B-SPLINES

A spline function of order M (degree M-1) is simply a piecewise polynomial $\underline{S}(u)$, with M-2 continuous derivatives at the knots or joints between the individual polynomials. The parametric variable u varies between an initial value u_o and some final value u_m as the curve is tracked.

More precisely, suppose that U denotes the set of real numbers $\{u_o,\ldots, u_m\}$ where $a=u_o<u_1<\ldots<u_{m-1}<u_m=b$. Now, let S represent the set of all functions given by

$$S = S(U) = S(u) \in C^{M-2}[a,b] , \qquad (2.1)$$

having the property that in each interval $[u_i,u_{i+1}]$, i=0,...,m-1, $\underline{S}(u)$ takes on the same values as a polynomial of degree M-1. Such functions are called splines of order M and satisfy the conditions:

1. $\underline{S}(u)$ is a polynomial of degree at most, M-1 on each interval $[u_i, u_{i+1}]$, i=0,...,m-1; and
2. $\underline{S}(u)$ and its first M-2 derivatives are continuous eveywhere.

The set of splines S, is a linear space. That is, given any two elements, any linear combination is also a member of the set S. This is important in order to determine a basis for S. In fact, there are many bases for S. Perhaps the most commonly used is the B-spline basis. An extension of the Bernstein basis [10, 11], the B-spline basis has been widely adopted because of its implicit localized effect. Characteristically, the B-spline basis is zero eveywhere except over M consecutive knot intervals. Gordon and Riesenfeld [12] refer to this finite nonzero span of the basis function as the support width. That is, the support width of the B-spline basis is always the interval $[u_i, u_{i+M}]$ which spans M segments (Figure 2.1).

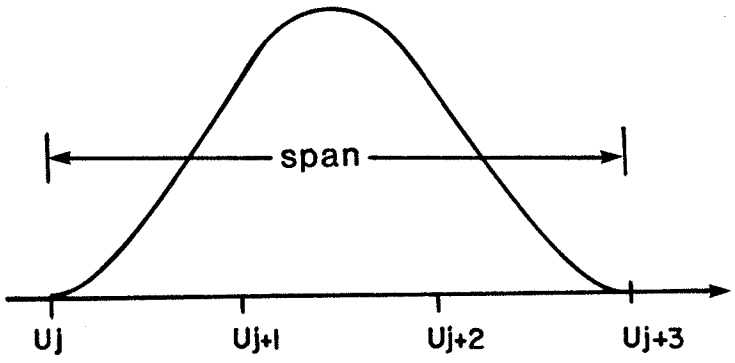

Figure 2.1: A single quadratic B-spline basis function of support width=3.

Cubic B-splines (M=4) with uniform knot sequences have been extensively used in curve and surface modelling primarily because of their ease of implementation. The uniform knot sequence is taken to be succesive integers given by

$$u_m = \{0,1,\ldots,m\} \tag{2.2}$$

or simply

$$u_i = i \ . \tag{2.3}$$

Let the functions $B_i(u)$ be the normalized uniform cubic B-spline basis functions. The normalizing condition suggest that at any particular value of u, the following must hold:

$$\sum_i B_i(u) = 1 \ . \tag{2.4}$$

This condition completely defines the basis and results in some useful properties which will be discussed in subsequent sections.

One of the most direct ways to define a curve using the cubic B-spline basis is to provide a finite number of points near which the curve is to pass. These points, denoted by

$\underline{V}$, are called <u>control vertices</u> and are meant to imply

$$\underline{V} = [V_x \; V_y] \quad \text{or} \quad \underline{V} = [V_x \; V_y \; V_z] \; , \tag{2.5}$$

in the case of two- and three-dimensional curves, respectively. Their interconnections form what is commonly referred to as the <u>control polygon</u>.

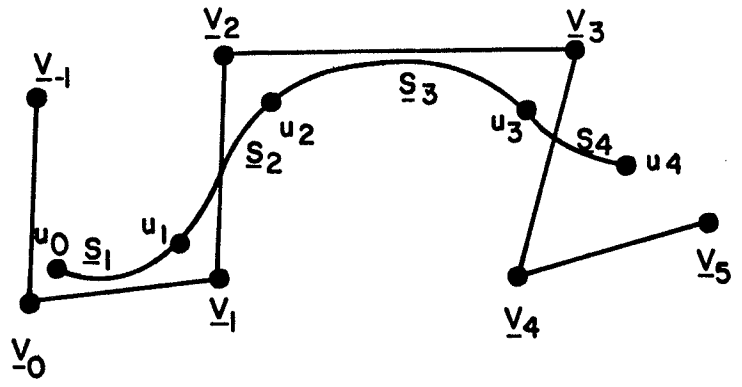

Figure 2.2: Cubic B-spline curve with control vertices $\underline{V}_{-1}, \ldots, \underline{V}_5$.

A vector-valued function can then be defined by both the control vertices and the uniform cubic B-spline basis functions as follows:

$$\underline{S}(u) = [X(u)\ Y(u)\ Z(u)]$$

$$= \left[\sum_{i=-1}^{m+1} V_{xi} B_i(u) \sum_{i=-1}^{m+1} V_{yi} B_i(u) \sum_{i=-1}^{m+1} V_{zi} B_i(u) \right] . \qquad (2.6)$$

In this manner, the individual x, y and z-coordinates can be determined as separate entities. Functions such as (2.6) are referred to as parametric cubic curves, being cubic functions of the parametric variable u. For the two-dimensional curve depicted in Figure 2.2,

$$\underline{S}(u) = \sum_{i=-1}^{5} \underline{V}_i B_i(u) \qquad u_0 \le u \le u_4 . \qquad (2.7)$$

The curve, $\underline{S}(u)$ is made up of four piecewise continuous segments. Each segment has associated with it four control vertices implying that each vertex exerts control on four localized segments. This is the result of the support width (equal to four) of the cubic B-spline basis function, $B_i(u)$. Moverover, in this form, the curve in Figure 2.2 only approximates the control polygon.

Since the basis function, $B_i(u)$, is zero everywhere except over four consecutive knot intervals, given by

$$[u_{i-2}, u_{i+2}] , \qquad (2.8)$$

a particular curve segment, $\underline{S}_i(u)$, bounded by the interval $[u_{i-1}, u_i]$, can be written as

$$\underline{S}_i(u) = \sum_{j=i-2}^{i+1} \underline{V}_j B_j(u) \ . \qquad (2.9)$$

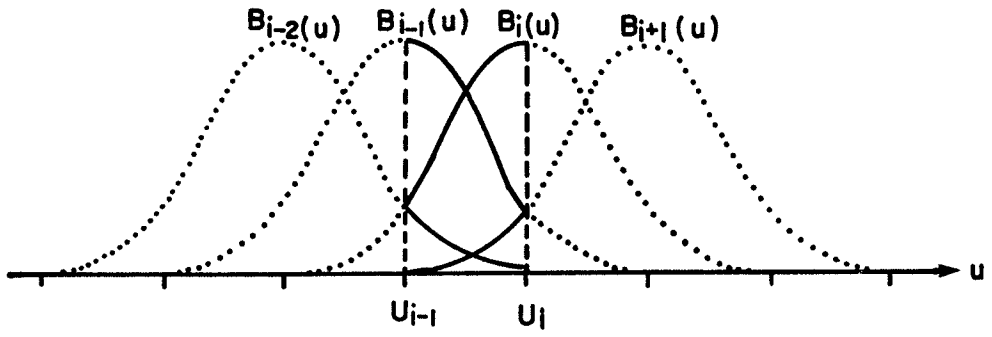

Figure 2.3: B-spline basis portions affecting $\underline{S}_i(u)$ on $[u_{i-1}, u_i]$.

However, only certain portions of the basis functions affect the construction of $\underline{S}_i(u)$, as Figure 2.3 illustrates. In fact, if the cubic B-spline basis functions are subdivided into smaller spans of single knot intervals as Figure 2.4[1] suggests, then $\underline{S}_i(u)$ may be written as

---

[1] Adapted from [13].

$$\underline{S}_i(u) = \underline{V}_{i-2} b_{-2}^{(i-2)}(u) + \underline{V}_{i-1} b_{-1}^{(i-1)}(u) + \underline{V}_i b_0^{(i)}(u) + \underline{V}_{i+1} b_1^{(i+1)}(u) \quad (2.10)$$

where $b_{-2}^{(i-2)}(u)$, $b_{-1}^{(i-1)}(u)$, $b_0^{(i)}(u)$ and $b_1^{(i+1)}(u)$ correspond to the portions of $B_{i-2}(u)$, $B_{i-1}(u)$, $B_i(u)$ and $B_{i+1}(u)$ defined on the interval $[u_{i-1}, u_i]$ (Figure 2.5).

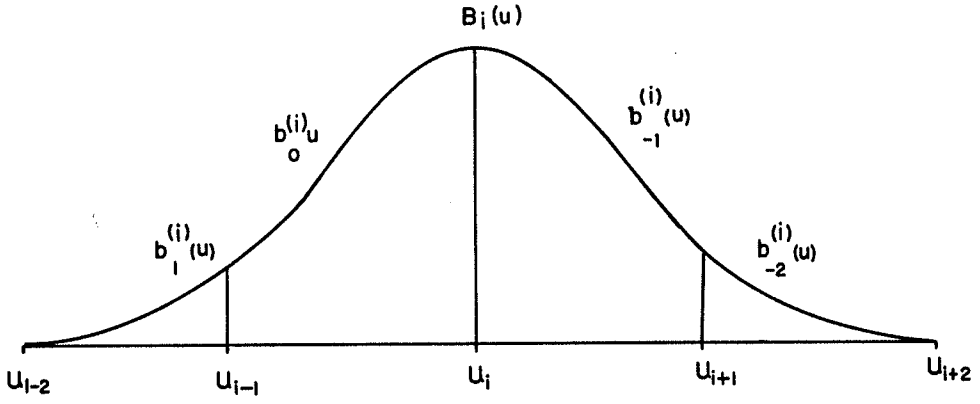

Figure 2.4: Subdivision of the uniform cubic B-spline basis function.

There is some question of validity in the subdivison of the cubic B-spline basis. Recall the set of set of cubic splines, for which $B_i(u)$ forms a basis, is a linear space. Thus, $B_i(u)$ is a member of that set. Therefore, it must satisfy the conditions:

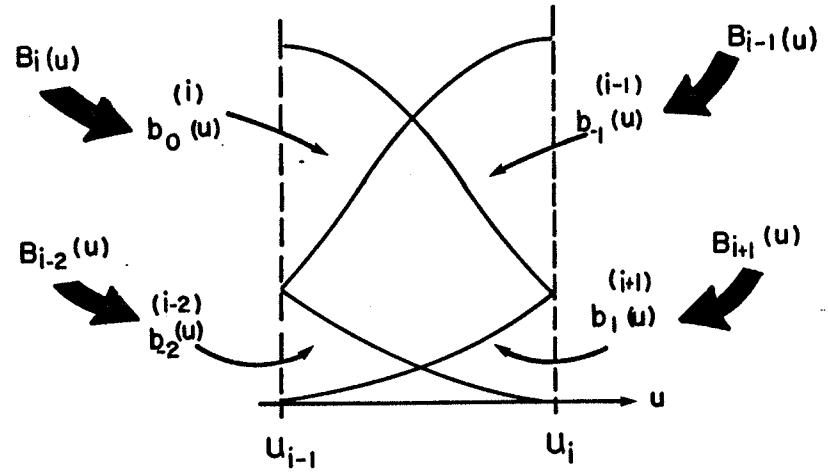

Figure 2.5: Cubic B-spline basis subdivison on $[u_{i-1}, u_i]$.

1. $B_i(u)$ is a polynomial of degree three at most on each interval $[u_{i-1},u_i]$; and
2. $B_i(u)$ and its first two derivatives are continuous everywhere.

Clearly, by the first condition, $b_{-2}^{(i)}(u)$, $b_{-1}^{(i)}(u)$, $b_0^{(i)}(u)$ and $b_1^{(i)}(u)$ agree with cubic polynomials on their respective intervals. Moreover, if the second condition is true of $B_i(u)$, then it must be true of the $b_r^{(i)}(u)$'s on their domain of definition. Thus, the linear combination in (2.10) is a valid representation for the curve segment, $\underline{S}_i(u)$.

To obtain the complete curve representation, $\underline{S}(u)$ can be expressed as a summation of curve segments. Recall that a particular curve segment $\underline{S}_i(u)$, is bounded by $[u_{i-1},u_i]$. This can be viewed as a parametric function which is zero

everywhere except over $[u_{i-1}, \quad u_i]$. Thus, the individual curve segments which comprise the curve can be considered orthogonal over the span of the parametric variable. That is,

$$\int_{u_o}^{u_m} \underline{S}_i(u)\, \underline{S}_j(u)\, du = 0 \qquad (i \neq j) \; . \tag{2.11}$$

As a consequence, $\underline{S}(u)$ can be represented as the sum of orthogonal curve segments. For the curve in Figure 2.2:

$$\underline{S}(u) = \sum_{1}^{4} \underline{S}_i(u) = \underline{S}_1(u) + \underline{S}_2(u) + \underline{S}_3(u) + \underline{S}_4(u) \; . \tag{2.12}$$

In terms of the subsectional basis functions, (2.12) becomes

$$\begin{aligned} \underline{S}(u) = {} & \underline{V}_{-1} b_{-2}^{(-1)} + \underline{V}_0 b_{-1}^{(0)} + \underline{V}_1 b_0^{(1)} + \underline{V}_2 b_1^{(2)} \\ & + \underline{V}_0 b_{-2}^{(0)} + \underline{V}_1 b_{-1}^{(1)} + \underline{V}_2 b_0^{(2)} + \underline{V}_3 b_1^{(3)} \\ & + \underline{V}_1 b_{-2}^{(1)} + \underline{V}_2 b_{-1}^{(2)} + \underline{V}_3 b_0^{(3)} + \underline{V}_4 b_1^{(4)} \\ & + \underline{V}_2 b_{-2}^{(2)} + \underline{V}_3 b_{-1}^{(3)} + \underline{V}_4 b_0^{(4)} + \underline{V}_5 b_1^{(5)} \; . \end{aligned} \tag{2.13}$$

Rewriting (2.13), results in

$$\begin{aligned}\underline{S}(u) = {} & \underline{V}_{-1}b_{-2}^{(-1)} + \underline{V}_0[b_{-2}^{(0)} + b_{-1}^{(0)}] + \underline{V}_1[b_{-2}^{(1)} + b_{-1}^{(1)} + b_0^{(1)}] \\ & + \underline{V}_2[b_{-2}^{(2)} + b_{-1}^{(2)} + b_0^{(2)} + b_1^{(2)}] + \underline{V}_3[b_{-1}^{(3)} + b_0^{(3)} + b_1^{(3)}] \\ & + \underline{V}_4[b_0^{(4)} + b_1^{(4)}] + \underline{V}_5 b_1^{(5)} \quad .\end{aligned} \tag{2.14}$$

Finally, substituting the B-spline basis functions for the subsectional basis functions yields:

$$\begin{aligned}\underline{S}(u) = {} & \underline{V}_{-1}B_{-1}(u) + \underline{V}_0B_0(u) + \underline{V}_1B_1(u) + \underline{V}_2B_2(u) \\ & + \underline{V}_3B_3(u) + \underline{V}_4B_4(u) + \underline{V}_5B_5(u) \\ = {} & \sum_{i=-1}^{5} \underline{V}_iB_i(u) \qquad u_0 \le u \le u_4 \quad .\end{aligned} \tag{2.15}$$

This is precisely the result given by (2.7). The multiplication of $\underline{V}_iB_i(u)$ in (2.15) should not be misinterpreted as being the strict product of $\underline{V}_i$ with $B_i(u)$ defined over its parametric domain. Rather, $\underline{V}_i$ is multiplied by that portion of $B_i(u)$ bounded by the parametric domain of the entire curve.

The individual cubic B-spline basis functions, $B_i(u)$, are indistinguishable from each other in form and differ only in the domain of their definition. This is due to the uniform knot sequence selected. For reasons of convenience we will dispense with the superscript notation of the subsectional B-spline basis functions and simply refer to the individual subbases as

$$b_r(u),\ r = -2,-1,0,1\ . \tag{2.16}$$

2.2 DERIVATION OF THE UNIFORM CUBIC B-SPLINE BASIS FUNCTIONS

Up until now, it was assumed that the cubic B-spline basis functions satisfy the conditions:

1. $B_i(u)$ is a polynomial of a maximum degree of three on each interval $[u_{i-1},u_i]$, specifically, $b_r(u)$ r=-2,-1,0,1; and
2. $B_i(u)$ and its first two derivatives are continuous everywhere.

We can utilize the above two conditions to determine the explicit form of the subsectional cubic B-spline basis, $b_r(u)$. Consider the two consecutive curve segments, $\underline{S}_i(u)$ and $\underline{S}_{i+1}(u)$, illustrated in Figure 2.6.

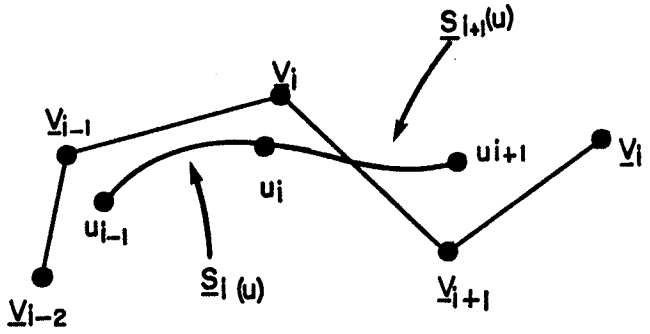

Figure 2.6: Two consecutive cubic B-spline segments.

Both curve segments, $\underline{S}_i(u)$ and $\underline{S}_{i+1}(u)$, are polynomials of degree three, at most. This is obvious since $\underline{S}_i(u)$ and $\underline{S}_{i+1}(u)$ are composed of linear combinations of cubic B-spline basis functions given by

$$\underline{S}_i(u) = \underline{V}_{i-2}b_{-2}(u) + \underline{V}_{i-1}b_{-1}(u) + \underline{V}_i b_0(u) + \underline{V}_{i+1}b_1(u) , \quad (2.17)$$

$$\underline{S}_{i+1}(u) = \underline{V}_{i-1}b_{-2}(u) + \underline{V}_i b_{-1}(u) + \underline{V}_{i+1}b_0(u) + \underline{V}_{i+2}b_1(u) . \quad (2.18)$$

Let each $b_r(u)$, $r=-2,-1,0,1$, valid on $[u_{i-1}, u_i]$, be described by cubic polynomials of the form

$$b_r(u) = a_r(u - u_{i-1})^3 + c_r(u - u_{i-1})^2 + d_r(u - u_{i-1}) + e_r , \quad r = -2,-1,0,1 . \quad (2.19)$$

Recall that the uniform knot sequence is given by consecutive integers (see (2.2)). For simplicity, (2.19) can be parametrized on a unit local domain.

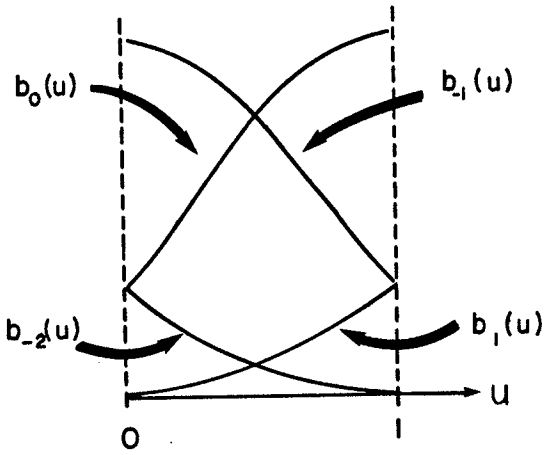

Figure 2.7: Uniform cubic B-spline basis segments on a unit domain.

Thus, (2.19) can be written as

$$b_r(u) = a_r u^3 + c_r u^2 + d_r u + e_r , \quad r = -2,-1,0,1 \text{ on } [0,1] . \quad (2.20)$$

The appropriate control vertices and the subsectional B-spline basis functions (defined by Figure 2.7) are combined to create a curve segment without loss of generality. This is further illustrated in Figure 2.8.

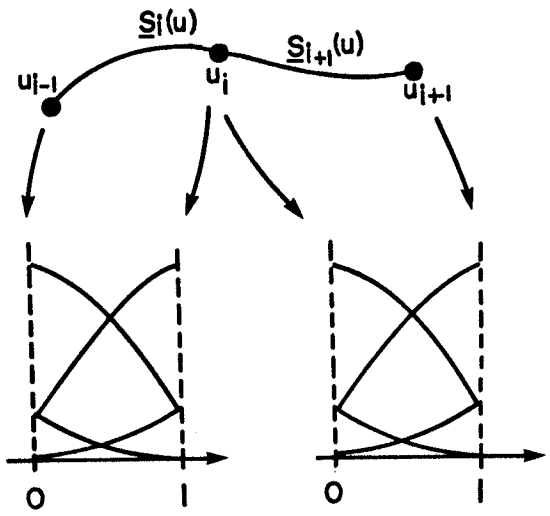

Figure 2.8: $\underline{S}_i(u)$ and $\underline{S}_{i+1}(u)$ and their subdivided B-spline basis.

$\underline{S}(u)$ and its first two parametric dervatives are continuous everywhere. Therefore, this order of continuity must hold at the point u which joins the individual curve segments. Thus,

$$\underline{S}_i(u_i) = \underline{S}_{i+1}(u_i) \ , \tag{2.21}$$

$$S'_i(u_i) = \underline{S}'_{i+1}(u_i) \ , \tag{2.22}$$

and

$$\underline{S}''_i(u_i) = S''_{i+1}(u_i) \ . \tag{2.23}$$

These requirements of positional, first derivative and

second derivative continuity between curve segments, along with the features shown in Figure 2.9, yields

$$\begin{aligned} &b_1(1) = b_0(0) \quad b_1'(1) = b_0'(0) \quad b_1''(1) = b_0''(0) \\ &b_0(1) = b_{-1}(0) \quad b_0'(1) = b_{-1}'(0) \quad b_0''(1) = b_{-1}''(0) \\ &b_{-1}(1) = b_{-2}(0) \quad b_{-1}'(1) = b_{-2}'(0) \quad b_{-1}''(1) = b_{-2}''(0) \,. \end{aligned} \tag{2.24}$$

Notice that the terms on the right-hand side of the equalities correspond to the curve segment $\underline{S}_{i+1}(u)$ on $[u_i, u_{i+1}]$, while the left-hand side entities are associated with $\underline{S}_i(u)$ on $[u_{i-1}, u_i]$.

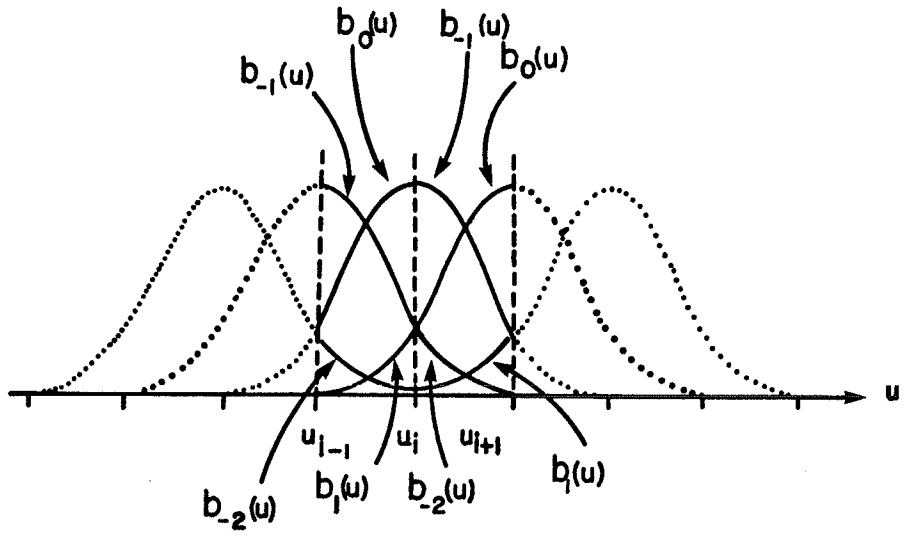

Figure 2.9: B-spline basis segments affecting $\underline{S}_i(u)$ and $\underline{S}_{i-1}(u)$.

In order to uniquely determine the sixteen coefficients, a_r, c_r, d_r and e_r in (2.20), sixteen constraint equations

must be determined. Even though (2.24) only reveals nine constraint equations, an additional six constraints can be obtained by reconsidering the support width of the cubic B-spline basis. Recall that $B_i(u)$ is zero except over four consecutive knot intervals. Referring to Figure 2.9, it is evident that

$$B_{i+2}(u)\Big|_{u=u_i} = b_1(0) = 0 \tag{2.25}$$

and

$$B_{i-2}(u)\Big|_{u=u_i} = b_{-2}(1) = 0 \ . \tag{2.26}$$

Moreover, the first and second derivatives must also be zero. Thus,

$$\begin{aligned} b_1'(0) &= 0 \quad b_1''(0) = 0 \\ b_{-2}'(1) &= 0 \quad b_{-2}''(1) = 0 \ . \end{aligned} \tag{2.27}$$

The additional equations (2.27) and (2.24), total fifteen equations in sixteen unknowns. Uniqueness can be attained by imposing the normalizing conditon of (2.4), namely,

$$\sum_{j=i-2}^{i+2} B_j(u)\Big|_{u=\alpha} = 1 \ . \tag{2.28}$$

Choosing a convenient location for evaluation, (2.28)

results in

$$b_1(0) + b_0(0) + b_{-1}(0) + b_{-2}(0) = 1 \ . \tag{2.29}$$

Thus, a completely determined set of constraints is given by

$$\begin{array}{lll}
b_{-2}(1) = 0 & b'_{-2}(1) = 0 & b''_{-2}(1) = 0 \\
b_{-1}(1) = b_{-2}(0) & b'_{-1}(1) = b'_{-2}(0) & b''_{-1}(1) = b''_{-2}(0) \\
b_0(1) = b_{-1}(0) & b'_0(1) = b'_{-1}(0) & b''_0(1) = b''_{-1}(0) \\
b_1(1) = b_0(0) & b'_1(1) = b'_0(0) & b''_1(1) = b''_0(0) \\
0 = b_1(0) & 0 = b'_1(0) & 0 = b''_1(0)
\end{array} \tag{2.30}$$

$$b_1(0) + b_0(0) + b_{-1}(0) + b_{-2}(0) = 1 \ .$$

Substituting (2.20) into (2.30) yields a system of linear equations in the unknown polynomial coefficients.

$$\begin{array}{lll}
a_{-2} + c_{-2} + d_{-2} + e_{-2} = 0 & 3a_{-2} + 2c_{-2} + d_{-2} = 0 & 6a_{-2} + 2c_{-2} = 0 \\
a_{-1} + c_{-1} + d_{-1} + e_{-1} = e_{-2} & 3a_{-1} + 2c_{-1} + d_{-1} = d_{-2} & 6a_{-1} + 2c_{-1} = 2c_{-2} \\
a_0 + c_0 + d_0 + e_0 = e_{-1} & 3a_0 + 2c_0 + d_0 = d_{-1} & 6a_0 + 2c_0 = 2c_{-1} \\
a_1 + c_1 + d_1 + e_1 = e_0 & 3a_1 + 2c_1 + d_1 = d_0 & 6a_1 + 2c_1 = 2c_0 \\
0 = e_1 & 0 = d_1 & 0 = 2c_1
\end{array} \tag{2.31}$$

$$e_{-2} + e_{-1} + e_0 = 1 \ .$$

In matrix notation,

$$
\begin{bmatrix}
 & & & & & & & & & 1 & 1 & 1 \\
1 & & & 1 & & & 1 & & & 1 & & \\
3 & & & 2 & & & 1 & & & & & \\
6 & & & 2 & & & & & & & & \\
 & -6 & & 2 & -2 & & & & & & & \\
 & & -6 & & 2 & -2 & & & & & & \\
 & & & -6 & & 2 & -2 & & & & & \\
 & & & & & & 2 & & & & & \\
 & -3 & & & -2 & & & 1 & -1 & & & \\
 & & -3 & & & -2 & & & 1 & -1 & & \\
 & & & -3 & & & -2 & & & 1 & -1 & \\
 & & & & & & & & & & 1 & \\
 & -1 & & & -1 & & & -1 & & & 1 & -1 \\
 & & -1 & & & -1 & & & -1 & & & 1 & -1 \\
 & & & -1 & & & -1 & & & -1 & & & 1 \\
 & & & & & & & & & & & & 1
\end{bmatrix}
\begin{bmatrix} a_{-2} \\ a_{-1} \\ a_0 \\ a_1 \\ c_{-2} \\ c_{-1} \\ c_0 \\ c_1 \\ d_{-2} \\ d_{-1} \\ d_0 \\ d_1 \\ e_{-2} \\ e_{-1} \\ e_0 \\ e_1 \end{bmatrix}
=
\begin{bmatrix} 1 \\ 0 \\ 0 \\ 0 \\ 0 \\ 0 \\ 0 \\ 0 \\ 0 \\ 0 \\ 0 \\ 0 \\ 0 \\ 0 \\ 0 \\ 0 \end{bmatrix} . \qquad (2.32)
$$

Solving the above system gives the explicit form of the subsectional B-spline basis functions defined on [0, 1] in Figure 2.7.

$$
\begin{aligned}
b_{-2}(u) &= (-u^3 + 3u^2 + 3u + 1)/6 , \\
b_{-1}(u) &= (3u^3 - 6u^2 + 4)/6 , \\
b_0(u) &= (-3u^3 + 3u^2 + 3u + 1)/6 , \\
b_1(u) &= u^3/6 .
\end{aligned} \qquad (2.33)
$$

2.3 SOME PROPERTIES OF THE UNIFORM CUBIC B-SPLINE BASIS

Uniform cubic B-splines exhibit many inherent properties which make them particularly desirable as curve and surface interpolants. The indigenous local control of the B-spline basis lends itself to isolated curve and surface modifications without disrupting the global structure. Again, this is due to to the support width (equal to four) of the uniform cubic B-spline basis. Thus, any alteration of a particular control vertex will influence, at most, four consecutive curve segments.

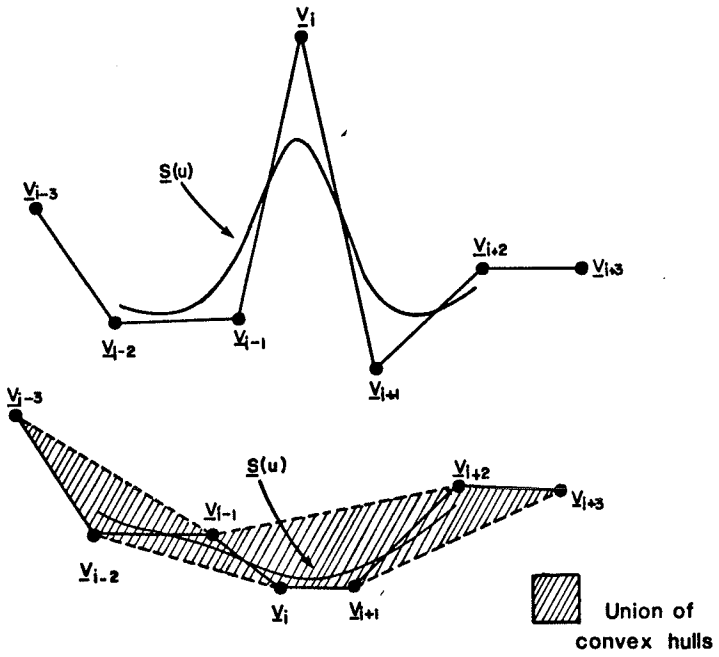

Figure 2.10: Local control and convex-hull properties.

This is evident by the movement of $\underline{V}_i$ in Figure 2.10. Recall that the normalizing constraint imposed on the

uniform cubic B-spline basis is given by

$$\sum_{r=-2}^{1} b_r(u)\Big|_{u=u_i} = 1 \ , \qquad (2.34)$$

As a result, the curve is forced to reside within the convex hull delineated by the extreme control vertices, that is, the union of the convex hulls of every four (in the case of cubics) consecutive control vertices [14].

2.4 INTERPOLATING WITH CUBIC B-SPLINE CURVES

An open cubic B-spline curve can be generated by combining piecewise cubic curve segments. Each curve segment $\underline{S}_i(u)$, is produced from a linear combination of subsectional basis functions defined parametrically over the length of the curve segment, where the coefficients are the corresponding control vertices.

$$\underline{S}_i(u) = \sum_{r=-2}^{1} \underline{V}_{i+r} b_r(u) \qquad 0 \le u \le 1 \qquad (2.35)$$

The end points of $\underline{S}_i(u)$ are parametrically defined by $\underline{S}_i(0)$ and $\underline{S}_i(1)$ and can be denoted by $\underline{p}_{i-1}$ and $\underline{p}_i$, respectively.

Suppose that $\underline{p}_{i-1}$ and $\underline{p}_i$ are known. It is possible to determine the four control vertices $\underline{V}$ such that the curve segment will pass through $\underline{p}_{i-1}$ and $\underline{p}_i$ provided there is a sufficient number of equations. However, in this

interpolation problem, there are two equations

$$\underline{P}_{i-1} = \underline{S}_i(0) = \underline{V}_{i-2}b_{-2}(0) + \underline{V}_{i-1}b_{-1}(0) + \underline{V}_i b_0(0) + \underline{V}_{i+1}b_1(0) \quad , \quad (2.36)$$

$$\underline{P}_i = \underline{S}_i(1) = \underline{V}_{i-2}b_{-2}(1) + \underline{V}_{i-1}b_{-1}(1) + \underline{V}_i b_0(1) + \underline{V}_{i+1}b_1(1) \quad , \quad (2.37)$$

and four unknowns. The problem is underdetermined. Consider interpolating an additional point $\underline{P}_{i+1}$ by appending a curve segment $\underline{S}_{i+1}(u)$. Proceeding as above, results in three equations

$$\underline{P}_{i-1} = \underline{S}_i(0) = \underline{V}_{i-2}b_{-2}(0) + \underline{V}_{i-1}b_{-1}(0) + \underline{V}_i b_0(0) + \underline{V}_{i+1}b_1(0) \quad , \quad (2.38)$$

$$\underline{P}_i = \underline{S}_i(1) = \underline{V}_{i-2}b_{-2}(1) + \underline{V}_{i-1}b_{-1}(1) + \underline{V}_i b_0(1) + \underline{V}_{i+1}b_1(1) \quad , \quad (2.39)$$

and

$$\underline{P}_{i+1} = \underline{S}_{i+1}(1) = \underline{V}_{i-1}b_{-2}(1) + \underline{V}_i b_{-1}(1) + \underline{V}_{i+1}b_0(1) + \underline{V}_{i+2}b_1(1) \quad , \quad (2.40)$$

and five unknowns. Substituting the appropriate values from Table 2.1, yields

$$\underline{P}_{i-1} = [\underline{V}_{i-2} + 4\underline{V}_{i-1} + \underline{V}_i]/6 \quad , \quad (2.41)$$

$$\underline{P}_i = [\underline{V}_{i-1} + 4\underline{V}_i + \underline{V}_{i+1}]/6 \quad , \quad (2.42)$$

and

$$\underline{P}_{i+1} = [\underline{V}_i + 4\underline{V}_{i+1} + \underline{V}_{i+2}]/6 \quad . \quad (2.43)$$

TABLE 2.1

Uniform Cubic Subsectional B-spline Basis Functions

Subsectional Basis Functions	u=0	u=1
$b_{-2}(u)=(-u^3+3u^2-3u+1)/6$	1/6	0
$b_{-1}(u)=(3u^3-6u^2+4)/6$	2/3	1/6
$b_0(u)=(-3u^3+3u^2+3u+1)/6$	1/6	2/3
$b_1(u)=u^3/6$	0	1/6

In general, interpolating k points requires k+2 appropriately situated control vertices or k+2 equations in k+2 unknowns.

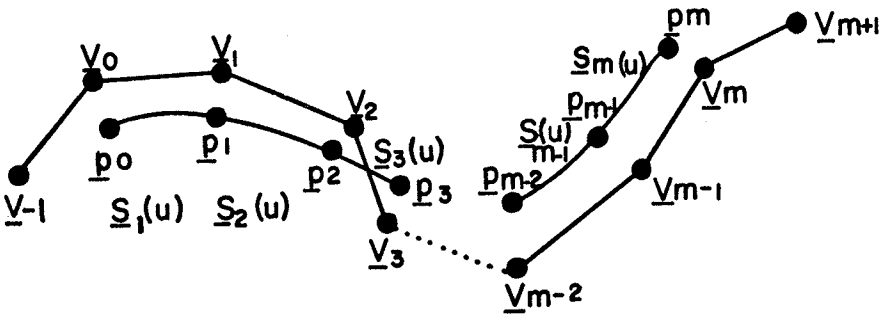

Figure 2.11: Open uniform cubic B-spline curve interpolating m+1 points.

Consider interpolating m+1 points given by

$$\underline{P}_i = [x_i \; y_i] \quad , \; i = 0,1,\ldots,m \; . \tag{2.44}$$

If the first and last control vertices, $\underline{V}_{-1}$ and $\underline{V}_{m+1}$, are arbitrarily chosen (thereby eliminating them from the unknowns), m+1 equations in m+1 unknowns can be generated as follows:

$$\underline{P}_0 = [\underline{V}_{-1} + 4\underline{V}_0 + \underline{V}_1]/6 \; , \tag{2.45}$$

$$\underline{P}_i = [\underline{V}_{i-1} + 4\underline{V}_i + \underline{V}_{i+1}]/6 \quad i = 1,2,\ldots,m-1 \; , \tag{2.46}$$

and

$$\underline{P}_m = [\underline{V}_{m-1} + 4\underline{V}_m + \underline{V}_{m+1}]/6 \; . \tag{2.47}$$

Since the <u>auxiliary</u> vertices, $\underline{V}_{-1}$ and $\underline{V}_{m+1}$ have been arbitrarily chosen, the above becomes

$$6\underline{P}_0 - \underline{V}_{-1} = 4\underline{V}_0 + V_1 \; , \tag{2.48}$$

$$6\underline{P}_i = \underline{V}_{i-1} + 4\underline{V}_i + \underline{V}_{i+1} \quad i = 1,2,\ldots,m-1 \; , \tag{2.49}$$

and

$$6\underline{P}_n - \underline{V}_{n+1} = \underline{V}_{n-1} + 4\underline{V}_n \; . \tag{2.50}$$

This has a unique solution given by

$$[\underline{V}] = [C]^{-1}[\underline{P}] \; , \tag{2.51}$$

where

$$[c] = \begin{bmatrix} 4 & 1 & & & \\ 1 & 4 & 1 & & \\ & \ddots & \ddots & \ddots & \\ & & 1 & 4 & 1 \\ & & & 1 & 4 \end{bmatrix}, \quad [\underline{V}] = \begin{bmatrix} \underline{V}_0 \\ \underline{V}_1 \\ \vdots \\ \underline{V}_{n-1} \\ \underline{V}_n \end{bmatrix}, \quad [\underline{p}] = \begin{bmatrix} 6\underline{p}_0 - \underline{V}_{-1} \\ 6\underline{p}_1 \\ \vdots \\ 6\underline{p}_{n-1} \\ 6\underline{p}_n - \underline{V}_{n+1} \end{bmatrix}. \qquad (2.52)$$

Using (2.35) in conjuction with the newly determined control vertices, each individual interpolating curve segment can be traced out over its parametric domain (see Figure 2.11). Since $\underline{V}_i$ and $\underline{p}_i$ may be of dimension two or three, the matrix multiplication in (2.51), and subsequently the curve generation, must be performed for each component.

The above interpolation scheme is adequate for most applications, however, it is obvious that the shapes of the curve segments $\underline{S}_1(u)$ and $\underline{S}_m(u)$ partially depend on the locations of the two auxiliary control vertices. This is evident from the end segment equations:

$$\underline{S}_1(u) = \underline{V}_{-1}b_{-2}(u) + \underline{V}_0 b_{-1}(u) + \underline{V}_1 b_0(u) + \underline{V}_2 b_1(u) , \qquad (2.53)$$

$$\underline{S}_m(u) = \underline{V}_{m-2}b_{-2}(u) + \underline{V}_{m-1}b_{-1}(u) + \underline{V}_m b_0(u) + \underline{V}_{m+1} b_1(u) . \qquad (2.54)$$

As the value of the parametric variable, u, approaches zero in (2.53) and approaches unity in (2.54), the respective curve segments become increasingly influenced by the auxiliary control vertices, $\underline{V}_{-1}$ and $\underline{V}_{m+1}$. This is entirely

due to the multiplying weight of the basis functions, $b_{-2}(u)$ and $b_1(u)$; Consequently, many unwanted artifacts can be generated by the improper placement of these auxiliary control vertices.

To alleviate the necessity of prescribing the location of the auxiliary vertices, additional constraints can be imposed upon the end curve segments. Such end constraints can be enforced in a variety of ways. Typically, this involves specifying certain parametric derivative conditions at the end points of the curve [15]. However, the motivation here is to extend this open curve concept to describe closed curves in which the specification of parametric derivative end constraints is unnecessary. In the following section these interpolation principles are applied to closed B-spline curves.

2.5 CLOSED B-SPLINE CURVE FORMULATION

In some instances it is necessary to be able to interpolate a set of points by a closed curve. Such techniques are useful in plotting contours or high-lighting boundaries between regions of different media. The closed uniform cubic B-spline can be constructed in much the same manner as the open B-spline curve.

Consider the closed uniform cubic B-spline curve of Figure 2.12. Such a curve can be obtained by over-lapping the control polygon ends of Figure 2.11, letting $\underline{p}_0=\underline{p}_m$. The

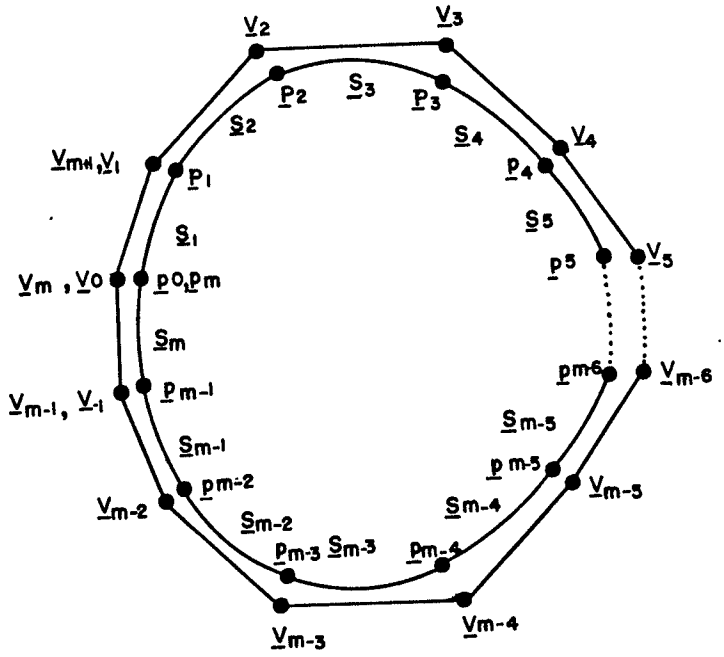

Figure 2.12: Closed uniform cubic B-spline curve interpolating m points.

closed curve of Figure 2.12 consists of m+3 control vertices: m distinct vertices and 3 auxiliary control vertices. To determine the m curve segments, m equations are required.

$$\begin{aligned} \underline{V}_0 + 4\underline{V}_1 + \underline{V}_2 &= 6\underline{P}_1 , \\ \underline{V}_{i-1} + 4\underline{V}_i + \underline{V}_{i+1} &= 6\underline{P}_i \quad i = 2,3,\ldots,m-1, \\ \underline{V}_{m-1} + 4\underline{V}_m + \underline{V}_{m+1} &= 6\underline{P}_m . \end{aligned} \tag{2.55}$$

To uniquely determine the m+3 control vertices in (2.55) requires three additional constraint equations. The way in

which the control polygon was constructed gives rise to

$$\begin{aligned} \underline{V}_{-1} &= \underline{V}_{m-1} , \\ \underline{V}_{0} &= \underline{V}_{m} , \\ \underline{V}_{1} &= \underline{V}_{m+1} . \end{aligned} \tag{2.56}$$

Combining (2.55) and (2.56) into a linear system of equations yields

$$\begin{bmatrix} 1 & & & & -1 \\ & 1 & & & -1 \\ & & 1 & 4 & 1 \\ & & & \ddots & \ddots & \ddots \\ & & & & 1 & 4 & 1 \\ & -1 & & & & & 1 \end{bmatrix} \begin{bmatrix} \underline{V}_{-1} \\ \underline{V}_{0} \\ \underline{V}_{1} \\ \vdots \\ \underline{V}_{m} \\ \underline{V}_{m+1} \end{bmatrix} = \begin{bmatrix} 0 \\ 0 \\ 6\underline{p}_{1} \\ \vdots \\ 6\underline{p}_{m} \\ 0 \end{bmatrix} . \tag{2.57}$$

The auxiliary control vertex constraint equations can be eliminated from the system by the following elementary row operations:

1. eliminate row 1 and column 1 by adding column 1 to column m+1,
2. eliminate row 2 and column 2 by adding column 2 to column m+2, and
3. eliminate row m+3 and column m+3 by adding column m+3 to column 3.

Thus, the matrix in (2.57) is reduced to

$$\begin{bmatrix} 4 & 1 & & & 1 \\ 1 & 4 & 1 & & \\ & \ddots & \ddots & \ddots & \\ & & 1 & 4 & 1 \\ 1 & & & 1 & 4 \end{bmatrix} \begin{bmatrix} \underline{V}_0 \\ \underline{V}_1 \\ \vdots \\ \underline{V}_{m-1} \\ \underline{V}_m \end{bmatrix} = \begin{bmatrix} 6\underline{p}_1 \\ 6\underline{p}_0 \\ \vdots \\ 6\underline{p}_{m-1} \\ 6\underline{p}_m \end{bmatrix} . \qquad (2.58)$$

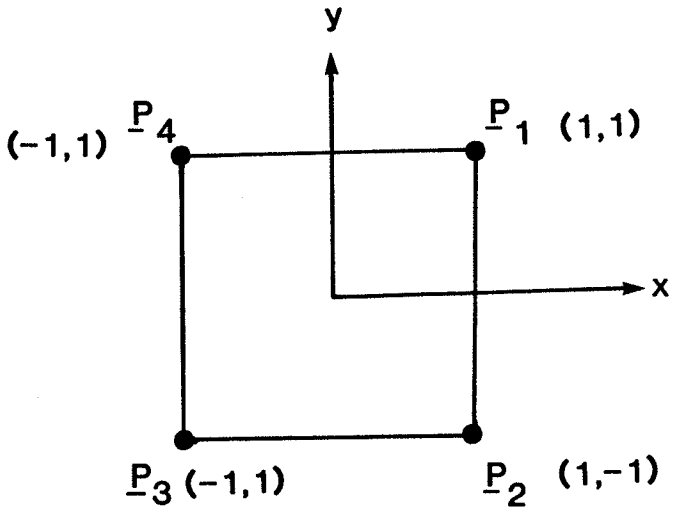

Figure 2.13: A unit square.

As an example, consider interpolating the corners the unit square given in Figure 2.13. The curve, which interpolates $\underline{p}_i$, i=1,..,4, consists of four curve segments

and four distinct control vertices.

$$
\begin{aligned}
\underline{S}_1(u) &= \underline{V}_{-1}b_{-2}(u) + \underline{V}_0 b_{-1}(u) + \underline{V}_1 b_0(u) + \underline{V}_2 b_1(u) \ , \\
\underline{S}_2(u) &= \underline{V}_0 b_{-2}(u) + \underline{V}_1 b_{-1}(u) + \underline{V}_2 b_0(u) + V_3 b_1(u) \ , \\
\underline{S}_3(u) &= \underline{V}_1 b_{-2}(u) + \underline{V}_2 b_{-1}(u) + \underline{V}_3 b_0(u) + \underline{V}_4 b_1(u) \ , \\
\underline{S}_4(u) &= \underline{V}_2 b_{-2}(u) + \underline{V}_3 b_{-1}(u) + \underline{V}_4 b_0(u) + \underline{V}_5 b_1(u) \ .
\end{aligned}
\tag{2.59}
$$

Evaluating the above at u=1 yields

$$
\begin{aligned}
\underline{S}_1(1) &= [\underline{V}_0 + 4\underline{V}_1 + \underline{V}_2]/6 = \underline{P}_1 \ , \\
\underline{S}_2(1) &= [\underline{V}_1 + 4\underline{V}_2 + \underline{V}_3]/6 = \underline{P}_2 \ , \\
\underline{S}_3(1) &= [\underline{V}_2 + 4\underline{V}_3 + \underline{V}_4]/6 = \underline{P}_3 \ , \\
S_4(1) &= [\underline{V}_3 + 4\underline{V}_4 + \underline{V}_5]/6 = \underline{P}_4 \ .
\end{aligned}
\tag{2.60}
$$

The curve segment equations in (2.60) generate three auxiliary control vertices, namely $\underline{V}_{-1}$, $\underline{V}_0$ and $\underline{V}_5$. However, for a closed curve that consists of four curve segments and interpolates four points, the control polygon must be closed. That is,

$$
\begin{aligned}
\underline{V}_0 &= \underline{V}_4 \ , \\
\underline{V}_5 &= \underline{V}_1 \ , \\
\underline{V}_{-1} &= \underline{V}_3 \ .
\end{aligned}
\tag{2.61}
$$

Combining (2.60) and (2.61) in matrix notation gives

$$\begin{bmatrix} 1 & & & -1 & & \\ & 1 & & & -1 & \\ 1 & 4 & 1 & & & \\ & 1 & 4 & 1 & & \\ & & 1 & 4 & 1 & \\ & & & 1 & 4 & 1 \\ & -1 & & & & 1 \end{bmatrix} \begin{bmatrix} \underline{V}_{-1} \\ \underline{V}_0 \\ \underline{V}_1 \\ \underline{V}_2 \\ \underline{V}_3 \\ \underline{V}_4 \\ \underline{V}_5 \end{bmatrix} = \begin{bmatrix} 0 \\ 0 \\ 6\underline{P}_1 \\ 6\underline{P}_2 \\ 6\underline{P}_3 \\ 6\underline{P}_4 \\ 0 \end{bmatrix} . \qquad (2.62)$$

Again, the auxiliary vertex constraint equations can be eliminated from the system using the following:

1. eliminate row 1 and column 1 by adding column 1 to column 5,
2. eliminate row 2 and column 2 by adding column 2 to column 6, and
3. eliminate row 7 and column 7 by adding column 7 to column 3.

This results in a system matrix consisting of the unknown distinct control vertices.

$$\begin{bmatrix} 4 & 1 & & 1 \\ 1 & 4 & 1 & \\ & 1 & 4 & 1 \\ 1 & & 1 & 4 \end{bmatrix} \begin{bmatrix} \underline{V}_1 \\ \underline{V}_2 \\ \underline{V}_3 \\ \underline{V}_4 \end{bmatrix} = \begin{bmatrix} 6\underline{P}_1 \\ 6\underline{P}_2 \\ 6\underline{P}_3 \\ 6\underline{P}_4 \end{bmatrix} . \qquad (2.63)$$

Upon inversion and multiplication, the four distinct control

vertices are given as

$$\begin{bmatrix} \underline{V}_1 \\ \underline{V}_2 \\ \underline{V}_3 \\ \underline{V}_4 \end{bmatrix} = \begin{bmatrix} 3/2 & 3/2 \\ 3/2 & -3/2 \\ -3/2 & -3/2 \\ -3/2 & 3/2 \end{bmatrix} . \tag{2.64}$$

Moreover, the auxiliary control vertices are given by the map vector

$$\begin{bmatrix} \underline{V}_{-1} \\ \underline{V}_0 \\ \underline{V}_5 \end{bmatrix} = \begin{bmatrix} \underline{V}_3 \\ \underline{V}_4 \\ \underline{V}_1 \end{bmatrix} = \begin{bmatrix} -3/2 & -3/2 \\ -3/2 & 3/2 \\ 3/2 & 3/2 \end{bmatrix} . \tag{2.65}$$

Substituting the values of the control vertices, in (2.64) and (2.65), along with the explicit form of the basis function segments, in Table 2.1, into the curve segment equations of (2.59) results in

$$\begin{aligned}
\underline{S}_1(u) &= \begin{bmatrix} X_1(u) \\ Y_1(u) \end{bmatrix} = \begin{bmatrix} (-2u^3 + 3u^2 + 3u - 2)/2 \\ (-3u^2 + 3u + 2)/2 \end{bmatrix} , \\
\underline{S}_2(u) &= \begin{bmatrix} X_2(u) \\ Y_2(u) \end{bmatrix} = \begin{bmatrix} (-3u^2 + 3u + 2)/2 \\ (2u^3 - 3u^2 - 3u + 2)/2 \end{bmatrix} , \\
\underline{S}_3(u) &= \begin{bmatrix} X_3(u) \\ Y_3(u) \end{bmatrix} = \begin{bmatrix} (2u^3 - 3u^2 - 3u + 2)/2 \\ (3u^2 - 3u - 2)/2 \end{bmatrix} , \\
\underline{S}_4(u) &= \begin{bmatrix} X_4(u) \\ Y_4(u) \end{bmatrix} = \begin{bmatrix} (3u^2 - 3u - 2)/2 \\ (-2u^3 + 3u^2 + 3u - 2)/2 \end{bmatrix} .
\end{aligned} \tag{2.66}$$

Thus, to generate the closed curve interpolating the corner

points of the unit square, the x- and y-coordinates of each curve segment are obtained by varying u, in (2.66), over its unit parametric domain. Note that the curve segments in Figure 2.14 do not form a perfect circle. Rather, they form a smooth piecewise cubic spline which is twice continuously differentiable everywhere (see equation (2.66)).

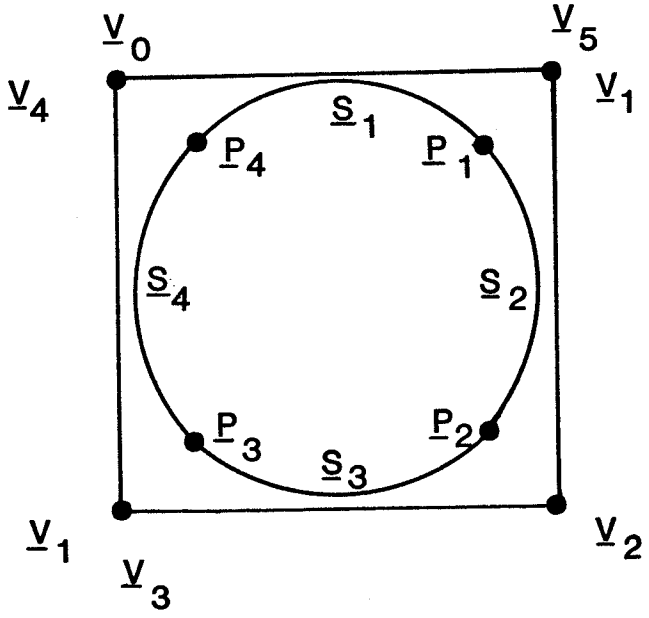

Figure 2.14: Closed uniform cubic B-spline interpolating a unit square.

Chapter III

PARAMETRIC UNIFORM BICUBIC B-SPLINE SURFACES

There have been several contributions to the field of surface modelling, specifically in surface representation (interpolation). Coons [5] developed methods of surface description based on the interconnection of surface patches called Coons patches. However, the Coons patch technique hinges upon the specification of parametric derivatives, in particular, patch corner cross-derivatives. Overhauser [16], followed by Brewer and Anderson [17], introduced the idea of parabolic blending, but these techniques only provide positional and first derivative continuity. Wu and Abel [18] presented an interpolating surface scheme based on lofting techniques [19]. The parallel planar curves which are generated, do not exhibit local control. Barsky [6], more recently, described a method of determining an interpolating surface through a prescribed network of points using bicubic B-splines. This method provides positional, first derivative, and second derivative continuity, and avoids the necessity of interpatch derivative specification. Barsky dealt with open B-spline surfaces which generate symmetric, positive-definite, tri-diagonal matrices. As a result, the method does not lend itself to

specify smooth closed bicubic surfaces, which characteristically generate nonsymmetric, positive-definite, sparse matrices.

A brief discussion on the open B-spline surface is presented in the following section to familiarize the reader with pertinent aspects of surface interpolation. Subsequent sections are devoted to the closed bicubic B-spline formulation.

3.1 INTERPOLATING WITH BICUBIC B-SPLINE SURFACES

The formulation of the uniform B-spline surfaces is an instinctive and logical extension of the uniform B-spline curve. The uniform cubic B-spline curve segment can be envisaged as the mapping of the one-dimensional space (u) onto the two- or three-dimensional Euclidean space, R^2 or R^3, respectively. In an analogous manner, a B-spline surface can be thought of as the mapping of the two-dimensional space (uv) onto the three-dimensional Euclidean space R^3 (see Figure 3.1).

A bicubic B-spline surface is formed by a linear combination of basis functions in much the same fashion as B-spline curves. However, for surfaces, the B-spline bases must be functions of two parametric variables, i.e. bivariate. This is realized by way of a tensor (cartesian, cross) product of univariate B-spline basis functions [20].

$$B_{i,j}(u,v) = B_i(u) \otimes B_j(v) = B_i(u)B_j(v) \ . \qquad (3.1)$$

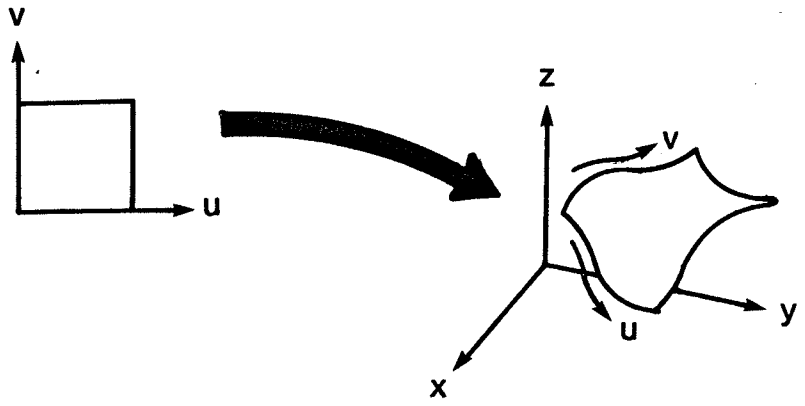

Figure 3.1: The mapping of the space (uv) onto the space R^3.

The functions $B_i(u)$ and $B_j(v)$ are simply the univariate basis functions used to express uniform cubic B-spline curves. Therefore, $B_{i,j}(u,v)$ must exhibit the convex-hull and localized control properties. Further, each basis function is zero everywhere except over four consecutive knot intervals in its respective parametric space, u or v. By expressing the basis function as a tensor product over the two-dimensional space (uv), the span of $B_{i,j}(u,v)$ can be visualized as a two-dimensional spread (see Figure 3.2).

This generalization to uniform bicubic surfaces requires that the control polygon of the B-spline curve be extended

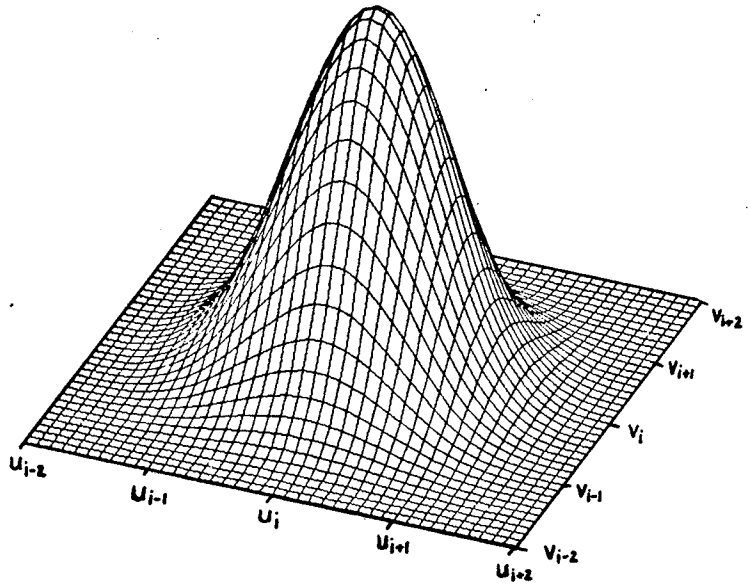

Figure 3.2: A bivariate uniform bicubic B-spline basis function.

to a control mesh, consisting of a net of control vertices.

$$\underline{V}_{i,j} = [Vx_{i,j}\ Vy_{i,j}\ Vz_{i,j}] \tag{3.2}$$

$$i = -1,0,\ldots,m,m+1 \quad j = -1,0,\ldots,n,n+1 \ .$$

As a result, a bicubic B-spline surface can be represented as a product of control vertices and B-spline basis functions (or portions thereof), defined over the parametric extent of the surface as follows:

$$\underline{P}(u,v) = \sum_i \sum_j \underline{V}_{i,j} B_i(u) B_j(v) \ . \tag{3.3}$$

A B-spline surface, $\underline{P}(u,v)$, is defined in a piecewise fashion, where each surface partition is called a patch, $\underline{P}_{i,j}(u,v)$. Moreover, each patch agrees with a cubic polynomial in each of its parametric directions. The entire surface, along with its first and second parametric derivatives, is continuous everywhere. This continuity is a direct consequence of the constraints placed on the univariate B-spline basis functions (see (2.30)). The result of this is the enforcement of interpatch continuity between adjoining surface patches (Figure 3.3).

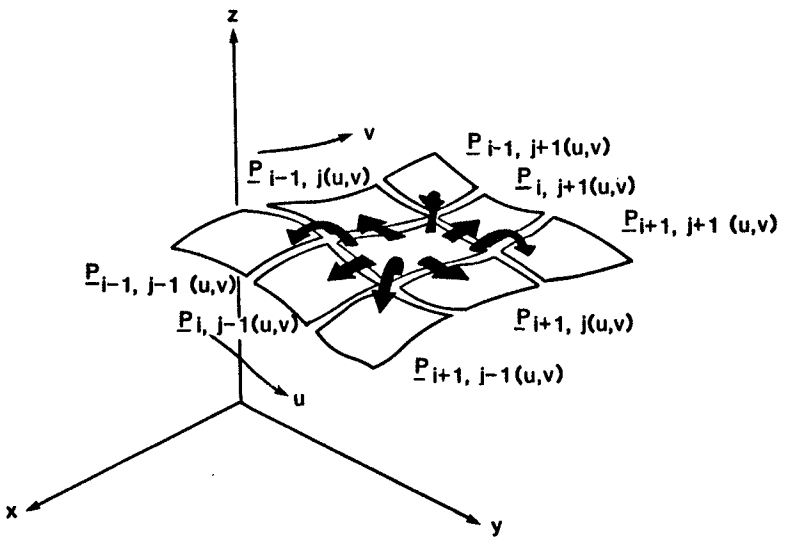

Figure 3.3: Continuity between adjoining surface patches.

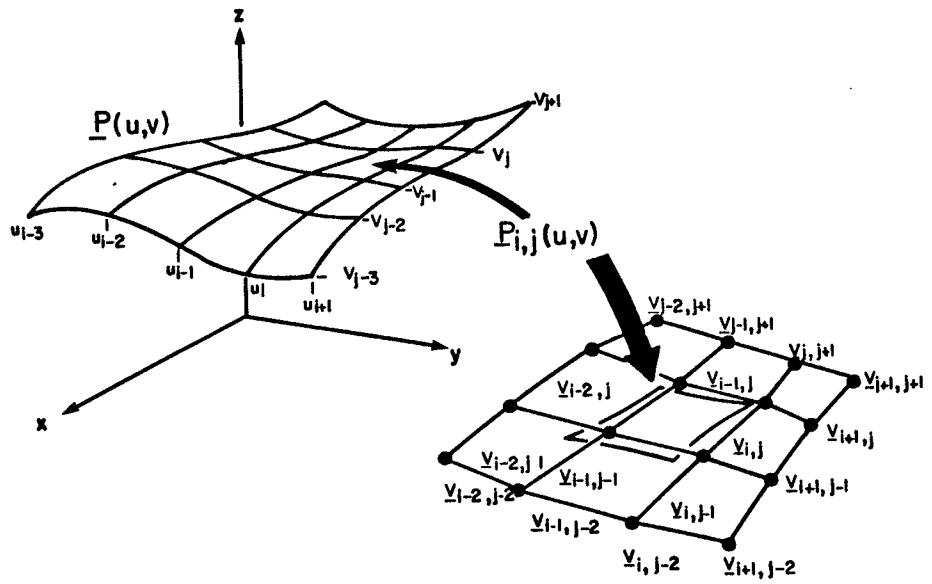

Figure 3.4: A single bicubic B-spline surface patch.

Only sixteen basis functions are nonzero over the parametric domain of any one surface patch region. For this reason, individual surface patches are influenced by sixteen control vertices (as Figure 3.4 suggests), implying that each vertex exerts control over sixteen surface patches. Thus, a surface patch, $\underline{P}_{i,j}(u,v)$ bounded by

$$u_{i-1} \leq u \leq u_i \ , \quad v_{i-1} \leq v \leq v_i \ , \tag{3.4}$$

can be defined exclusively by sixteen control vertices and

sixteen basis functions.

$$\underline{P}_{i,j}(u,v) = \sum_{r=-2}^{1} \sum_{s=-2}^{1} \underline{V}_{i+r,j+s} B_{i+r}(u) B_{j+s}(v) \ . \qquad (3.5)$$

Recall that only specific subsections of the univariate B-spline basis functions affect the construction of a B-spline curve segment. Extending this notion to the bivariate patch structure, (3.5) can be rewritten such that it utilizes the subsectional basis functions defined on the unit parametric domain of the patch. Thus,

$$B_{i+r}(u) B_{j+s}(v) \ , \qquad (3.6)$$

on $u_{i-1} \leq u \leq u_i$, $v_{j-1} \leq v \leq v_j$ becomes

$$b_r(u) b_s(v) \ , \qquad (3.7)$$

parametrized on $0 \leq u \leq 1$, $0 \leq v \leq 1$. Therefore, (3.5) can be represented as

$$\underline{P}_{i,j}(u,v) = \sum_{r=-2}^{1} \sum_{s=-2}^{1} \underline{V}_{i+r,j+s} b_r(u) b_s(v) \ . \qquad (3.8)$$

Suppose that the patch representation in (3.8) is employed to interpolate four rectangularly arranged points in R^3. With difficulty, the sixteen control vertices, combined

with sixteen basis functions, can be oriented in an attempt to allow the corners of the generated patch to interpolate the four points. However, this would lead to little success. Clearly, there is a need to explicitly define the patch corners in terms of the control vertices.

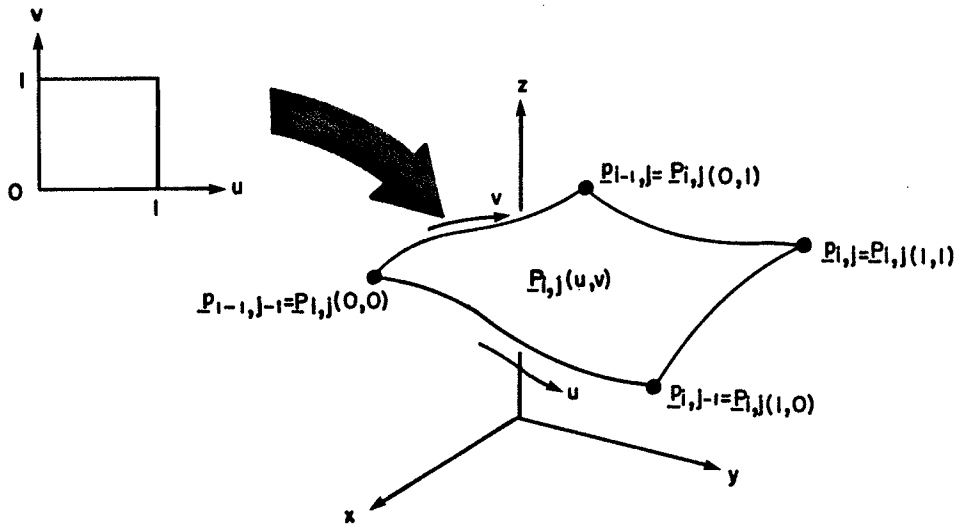

Figure 3.5: Corner point correspondence with a single bicubic patch.

A single patch, $\underline{P}_{i,j}(u,v)$, can be viewed as the mapping of the two-dimensional unit parametric space ($0 \leq u \leq 1$, $0 \leq v \leq 1$) onto the three-dimensional patch in R^3 (Figure 3.5). Consequently, expressions for the four corner points of the patch can be determined by evaluating the patch equation in (3.8) at the parametric extremes. Letting the

patch corners coalesce to the four points to be interpolated yields

$$\underline{P}_{i-1,j-1} = \underline{P}_{i,j}(0,0) \ , \quad \underline{P}_{i,j-1} = \underline{P}_{i,j}(1,0) \ ,$$
$$\underline{P}_{i-1,j} = \underline{P}_{i,j}(0,1) \ , \quad \underline{P}_{i,j} = \underline{P}_{i,j}(1,1) \ . \tag{3.9}$$

Utilizing the subsectional basis function values in Table 2.1 along with (3.9), the known points to be interpolated can be formulated in terms of the sixteen unknown control vertices.

$$\begin{aligned}
\underline{P}_{i-1,j-1} &= [\underline{V}_{i-2,j-2} + 4\underline{V}_{i-1,j-2} + \underline{V}_{i,j-2} + 4\underline{V}_{i-2,j-1} + 16\underline{V}_{i-1,j-1} + 4\underline{V}_{i,j-1} + \underline{V}_{i-2,j} \\
&\qquad + 4\underline{V}_{i-1,j} + \underline{V}_{i,j}]/36 \ , \\
\underline{P}_{i,j-1} &= [\underline{V}_{i-1,j-2} + 4\underline{V}_{i,j-2} + \underline{V}_{i+1,j-2} + 4\underline{V}_{i-1,j-1} + 16\underline{V}_{i,j-1} + 4\underline{V}_{i+1,j-1} + \underline{V}_{i-1,j} \\
&\qquad + 4\underline{V}_{i,j} + \underline{V}_{i+1,j}]/36 \ , \\
\underline{P}_{i-1,j} &= [\underline{V}_{i-2,j-1} + 4\underline{V}_{i-1,j-1} + \underline{V}_{i,j-1} + 4\underline{V}_{i-2,j} + 16\underline{V}_{i-1,j} + 4\underline{V}_{i,j} + \underline{V}_{i-2,j+1} \\
&\qquad + 4\underline{V}_{i-1,j+1} + \underline{V}_{i,j+1}]/36 \ , \\
\underline{P}_{i,j} &= [\underline{V}_{i-1,j-1} + 4\underline{V}_{i,j-1} + \underline{V}_{i+1,j-1} + 4\underline{V}_{i-1,j} + 16\underline{V}_{i,j} + 4\underline{V}_{i+1,j} + \underline{V}_{i-1,j+1} \\
&\qquad + 4\underline{V}_{i,j+1} + \underline{V}_{i+1,j+1}]/36 \ .
\end{aligned} \tag{3.10}$$

Admittedly, there is no hope of determining the sixteen unknown control vertices with just four equations.

Consider concatenating a network of surface patches into a rectangular arrangement of m by n patches. Again, the

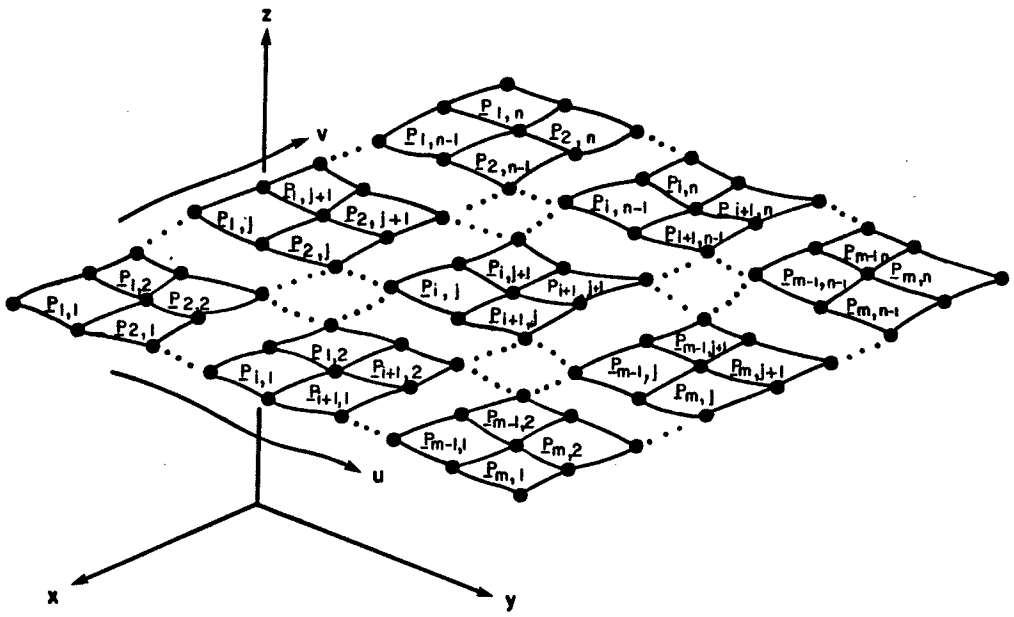

Figure 3.6: Surface made up of m by n patches.

patch corners are constrained to interpolate a network of points. However, for a multi-patch grouping, each patch shares at least three corner points between adjacent patches (Figure 3.6). For example, the parametric location of u=1, v=1, on the patch $\underline{P}_{i,j}(u,v)$, is identical to

$$\underline{P}_{i+1,j}(u,v)\Big|_{u=0,v=1} = \underline{P}_{i,j+1}(u,v)\Big|_{u=1,v=0} = \underline{P}_{i+1,j+1}(u,v)\Big|_{u=0,v=0} . \qquad (3.11)$$

Moreover, since there are (mn) patches, the number of distinct corner points is:

1. (mn) points corresponding to $\underline{P}_{i,j}(1,1)$ for i=1,...,m, j=1,...,n.

2. (m) points corresponding to $\underline{P}_{i,j}(1,0)$ for i=1,...,m, j=1.

3. (n) points corresponding to $\underline{P}_{i,j}(0,1)$ for i=1,j=1,...,n.

4. 1 point corresponding to $\underline{P}_{i,j}(0,0)$ for i=1,j=1.

Since the interpolation capability of the surface is equal to the number of distinct corner points available, the entire surface can be employed to interpolate a network of points, given by

$$\underline{P}_{i,j} \quad i = 0,1,\ldots,m \quad j = 0,1,\ldots,n \,. \tag{3.12}$$

These points can then be expressed in terms of the control vertices and B-spline basis functions by evaluating the corresponding surface patches at the appropriate corners.

$$\begin{aligned}
\underline{P}_{i,j} &= \underline{P}_{i,j}(1,1) = \sum_{r=-2}^{1}\sum_{s=-2}^{1} \underline{V}_{i+r,j+s} b_r(1) b_s(1) && i = 1,2,\ldots,m \quad j = 1,2,\ldots,n \,, \\
\underline{P}_{i,j-1} &= \underline{P}_{i,j}(1,0) = \sum_{r=-2}^{1}\sum_{s=-2}^{1} \underline{V}_{i+r,j+s} b_r(1) b_s(1) && i = 1,2,\ldots,m \quad j = 1 \,, \\
\underline{P}_{i-1,j} &= \underline{P}_{i,j}(0,1) = \sum_{r=-2}^{1}\sum_{s=-2}^{1} \underline{V}_{i+r,j+s} b_r(0) b_s(1) && i = 1 \quad\quad\; j = 1,2,\ldots,n \,, \\
\underline{P}_{i-1,j-1} &= \underline{P}_{i,j}(0,0) = \sum_{r=-2}^{1}\sum_{s=-2}^{1} \underline{V}_{i+r,j+s} b_r(0) b_s(0) && i = 1 \quad\quad\; j = 1 \,.
\end{aligned} \tag{3.13}$$

A close inspection of the above reveals that to support an interconnection of m by n patches (interpolating (m+1)(n+1) points), a control mesh of (m+3)(n+3) unknown control

vertices is required.

$$\underline{V}_{i,j} \quad i = -1,0,1,\ldots,m,m+1 \quad j = -1,0,1,\ldots,n,n+1 \; . \qquad (3.14)$$

Unfortunately, the patch-corner evaluations in (3.13) only generate (m+1)(n+1) equations. To obtain a completely determinable system an additional

$$(m + 3)(n + 3) - (m + 1)(n + 1) = 2m + 2n + 8 \qquad (3.15)$$

equations are necessary. These (2m+2n+8) supplementary equations are realized by introducing boundary conditions which constrain the periphery of the surface. Typically, this boundary enforcement is accomplished by specifying certain partial parametric derivatives about the surface perimeter.

Since a lengthy discussion in derivative boundary constraints is not beneficial to the clarification of closed bicubic surface formulation, the reader is referred to Barsky [15] on that matter.

3.2 CLOSED BICUBIC B-SPLINE SURFACE FORMULATION

Closed bicubic B-spline surfaces embody many of the interpolation techniques outlined in the previous section. Such surfaces can be implemented to interpolate a prescribed closed network of points in R^3. As a consequence of this, the control mesh, ordinarily unconnected, must be transformed to a totally connected or closed form. This control structure is what differentiates the formulation of closed surfaces from the conventional unnconnected surface.

By proper manipulation of the individual control vertices, sufficient constraints can be introduced to guarantee positional, first derivative, and second derivative continuity. This is attained in the absence of explicit boundary derivative specifications. The control vertex constraints, combined with the patch-corner interpolation capability, yield a determinable system of equations in the unknown control vertices.

In the preceding section, it was established that m by n interconnected surface patches had a capacity to interpolate (m+1)(n+1) points. This was accomplished by allowing the distinct corner patches to coalesce with the points to be interpolated. This concept can be extended to closed bicubic B-spline surfaces.

3.2.1 Closed Surface Patch Arrangement

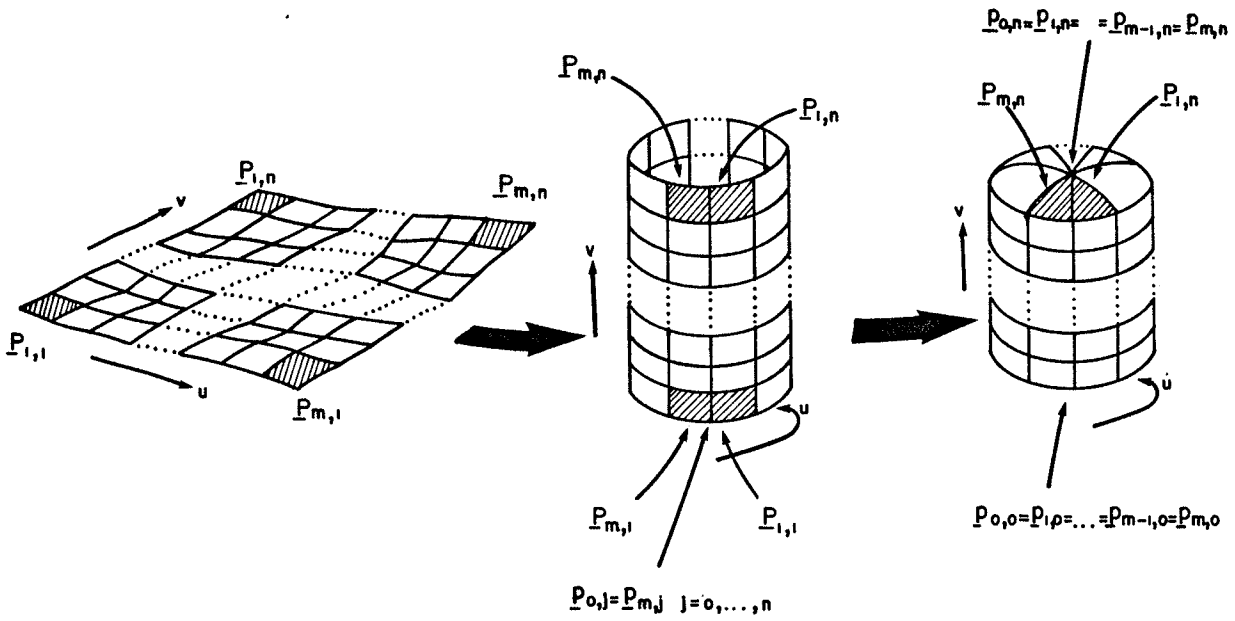

Figure 3.7: The transformation of m by n surface patches.

Consider the interconnection of m by n patches illustrated in Figure 3.6. Recall that because of the availabilty of the (m+1)(n+1) distinct patch-corner points, the surface can interpolate a network of rectangularly arranged points given by

$$\underline{P}_{i,j} \quad i = 0,1,\ldots,m \quad j = 0,1,\ldots,n \; . \tag{3.16}$$

Clearly, the problem at hand is how to interlink the m by n

surface patches to form a smooth impenetrable surface shell while interpolating a closed network of points. In the preceding discussion regarding closed cubic curves, it was demonstrated that a closed curve could be assembled by joining the end points of an open curve. Similarly, the unconnected m by n surface patches can be fastened together, producing a cylinder-like orientation (Figure 3.7). This transformation is accomplished by letting

$$\underline{P}_{0,j} = \underline{P}_{m,j} \quad j = 0,1,\ldots,n \; . \tag{3.17}$$

The merger of boundary surface patches achieves closure (geometrically) in the parametric u-direction, but the surface structure still remains open about the v extremes. This can be remedied by pinching-off the open boundary extremes in the following manner:

$$\underline{P}_{1,0} = \underline{P}_{2,0} = \cdots = \underline{P}_{m-1,0} = \underline{P}_{m,0} \; , \tag{3.18}$$

and

$$\underline{P}_{1,n} = \underline{P}_{2,n} = \cdots = \underline{P}_{m-1,n} = \underline{P}_{m,n} \; . \tag{3.19}$$

The effect of the surface closure reduces the availability of distinct patch-corner points for interpolation. That is,

1. $(n+1)$ corner points are eliminated by the introduction of (3.17), and
2. $2(m-1)$ corner points are eliminated by the introduction of (3.18) and (3.19).

This results in

$$(m + 1)(n + 1) - (n + 1) - 2(m - 1) = (m)(n - 1) + 2 , \quad (3.20)$$

distinct points useable for interpolation.

The patch corners can be expressed in terms of the subsectional B-spline basis functions and the $(m+3)(n+3)$ control vertices, resulting in $(m+1)(n+1)$ equations.

$$\begin{aligned}
\underline{P}_{i,j} &= \underline{P}_{i,j}(1,1) = \sum_{r=-2}^{1}\sum_{s=-2}^{1} \underline{V}_{i+r,j+s} b_r(1) b_s(1) \quad i = 1,2,\ldots,m \quad j = 1,2,\ldots,n , \\
\underline{P}_{i,j-1} &= \underline{P}_{i,j}(1,0) = \sum_{r=-2}^{1}\sum_{s=-2}^{1} \underline{V}_{i+r,j+s} b_r(1) b_s(1) \quad i = 1,2,\ldots,m \quad j = 1 , \\
\underline{P}_{i-1,j} &= \underline{P}_{i,j}(0,1) = \sum_{r=-2}^{1}\sum_{s=-2}^{1} \underline{V}_{i+r,j+s} b_r(0) b_s(1) \quad i = 1 \quad j = 1,2,\ldots,n , \\
\underline{P}_{i-1,j-1} &= \underline{P}_{i,j}(0,0) = \sum_{r=-2}^{1}\sum_{s=-2}^{1} \underline{V}_{i+r,j+s} b_r(0) b_s(0) \quad i = 1 \quad j = 1 .
\end{aligned} \quad (3.21)$$

Enforcing the constraints in (3.17), (3.18), and (3.19) only serves to alter the left-hand side of $(m)(n-1)+2$ of the

(m+1)(n+1) patch corner equations in (3.21). There is no reduction in the number of equations, only in the number of points available for interpolation.

Examining the equations in (3.21), which are directly affected by the constraints, it becomes evident that equating patch-corner points only ensures positional continuity. No provisions are made to guarantee any derivative continuity. For example, the corner point equations for $\underline{P}_{0,j}$ and $\underline{P}_{m,j}$, where j=0,1,...,n, are given by

$$\begin{aligned} \underline{P}_{0,0} &= \sum_{r=-2}^{1} \sum_{s=-2}^{1} \underline{V}_{-1+r,j+s} b_r(0) b_s(0) \ , \\ \underline{P}_{0,j} &= \sum_{r=-2}^{1} \sum_{s=-2}^{1} \underline{V}_{-1+r,j+s} b_r(0) b_s(1) \quad j = 1,2,\ldots,n \ , \end{aligned} \tag{3.22}$$

and

$$\begin{aligned} \underline{P}_{m,0} &= \sum_{r=-2}^{1} \sum_{s=-2}^{1} \underline{V}_{m+r,1+s} b_r(1) b_s(0) \ , \\ \underline{P}_{m,j} &= \sum_{r=-2}^{1} \sum_{s=-2}^{1} \underline{V}_{m+r,j+s} b_r(1) b_s(1) \quad j = 1,2,\ldots,n \ . \end{aligned} \tag{3.23}$$

Applying the constraint in (3.17) results in

$$\begin{aligned} \underline{P}_{m,0} &= \sum_{r=-2}^{1}\sum_{s=-2}^{1} \underline{V}_{l+r,l+s} b_r(0)b(0) = \sum_{r=-2}^{1}\sum_{s=-2}^{1} \underline{V}_{m+r,l+s} b_r(1)b_s(0) , \\ \underline{P}_{m,j} &= \sum_{r=-2}^{1}\sum_{s=-2}^{1} \underline{V}_{l+r,j+s} b_r(0)b_s(1) = \sum_{r=-2}^{1}\sum_{s=-2}^{1} \underline{V}_{m+r,j+s} b_r(1)b_s(1) \quad j = 1,2,\ldots,n . \end{aligned} \tag{3.24}$$

Differentiating the above with respect to the parametric variable u in an attempt to promote first derivative continuity, yields

$$\begin{aligned} \sum_{r=-2}^{1}\sum_{s=-2}^{1} \underline{V}_{l+r,l+s} b'_r(0)b_s(0) &= \sum_{r=-2}^{1}\sum_{s=-2}^{1} \underline{V}_{m+r,l+s} b'_r(1)b_s(0) , \\ \sum_{r=-2}^{1}\sum_{s=-2}^{1} \underline{V}_{l+r,j+s} b'_r(0)b_s(1) &= \sum_{r=-2}^{1}\sum_{s=-2}^{1} \underline{V}_{m+r,j+s} b'_r(1)b_s(1) \quad j = 1,2,\ldots,n . \end{aligned} \tag{3.25}$$

Clearly, (3.25) only holds for certain control vertices. Therefore, it is possible that the control vertices can be determined such that first derivative continuity is preserved across the merger of the boundary surface patches. This same idea can be extended to incorporate the equality of the second derivative as well. Thus, if (2m+2n+8) boundary conditions are secured by way of equating first and second patch-corner derivative equations, then such constraints can be combined with the (m+1)(n+1) patch-corner point equations to yield a completely determinable system of

(m+3)(n+3) equations in (m+3)(n+3) unknown control vertices.

$$[\underline{V}] = [C]^{-1}[\underline{p}] \ . \qquad (3.26)$$

However, this boundary derivative specification is precisely what we wish to avoid. In the following section, the problem of determining an appropriate control vertex structure which inherently guarantees positional, first derivative, and second derivative continuity everywhere upon the interpolating surface is addressed.

3.2.2 Closed Surface Control Vertex Structure

It is apparent from the preceding section that the control vertex structure, which supports the bicubic surface, plays a major role in securing the continuity between surface patches. This is particularly true of the patch boundaries that merge to constitute the closed bicubic surface. The obvious question is: How can the control vertices be utilized to ensure generating a smooth continuous surface without having to resort to explicit boundary derivative specification?

3.2.2.1 Continuity at the u-Parameter Extremes

Recall that m by n bicubic surface patches require the

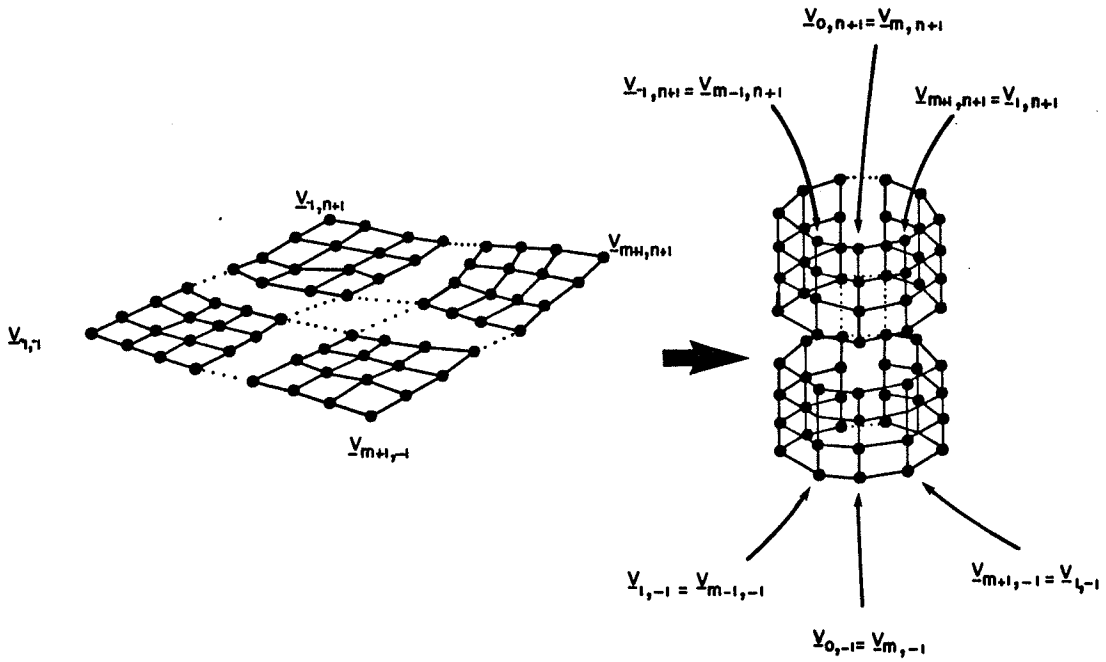

Figure 3.8: Control mesh overlap.

support of (m+3)(n+3) control vertices, given by

$$\underline{V}_{i,j} \quad i = -1,0,1,\ldots,m,m+1 \quad j = -1,0,1,\ldots,n,n+1 \ . \tag{3.27}$$

Suppose that the parametric extents of the control mesh are overlapped in a manner similar to that illustrated in the discussion on closed cubic curves (Figure 3.8). That is,

$$\begin{aligned} \underline{V}_{0,j} &= \underline{V}_{m,j} \ , \\ \underline{V}_{-1,j} &= \underline{V}_{m-1,j} \ , \quad j = -1,0,1,\ldots,n,n+1 \ . \\ \underline{V}_{m+1,j} &= \underline{V}_{1,j} \ , \end{aligned} \tag{3.28}$$

This should guarantee positional, first derivative, and second derivative continuity on the surface in the parmetric u-direction, as it did for the closed curve.

To illustrate this, reconsider the surface patch equations which are affected by the patch merger (Figure 3.7).

$$\underline{P}_{l,j}(u,v) = \sum_{r=-2}^{1} \sum_{s=-2}^{1} \underline{V}_{l+r,j+s} b_r(u) b_s(v) \quad j = 1,2,\ldots,n \ , \quad (3.29)$$

and

$$\underline{P}_{m,j}(u,v) = \sum_{r=-2}^{1} \sum_{s=-2}^{1} \underline{V}_{m+r,j+s} b_r(u) b_s(v) \quad j = 1,2,\ldots,n \ . \quad (3.30)$$

With the (n+1) corner point constraints introduced in the previous section (3.18), only positional continuity is ensured. The effect of the 3(n+3) control vertex constraints in (3.28) upon the derivative continuity between the boundary patches can be exemplified by differentiating (3.29) and (3.30) with respect to u, yielding

$$\frac{\partial \underline{P}_{l,j}(u,v)}{\partial u} = \sum_{r=-2}^{1} \sum_{s=-2}^{1} \underline{V}_{l+r,j+s} b'_r(u) b_s(v) \quad j = 1,2,\ldots,n \ , \quad (3.31)$$

and

$$\frac{\partial \underline{P}_{m,j}(u,v)}{\partial u} = \sum_{r=-2}^{1} \sum_{s=-2}^{1} \underline{V}_{m+r,j+s} b'_r(u) b_s(u) \quad j = 1,2,\ldots,n \ . \tag{3.32}$$

respectively. Evaluating (3.29) at u=0, and (3.30) at u=1, and then expanding, yields

$$\begin{aligned}
\frac{\partial \underline{P}_{-1,j}(u,v)}{\partial u}\Big|_{u=0} &= [\underline{V}_{-1,j-2} b'_{-2}(0) + \underline{V}_{0,j-2} b'_{-1}(0) + \underline{V}_{1,j-2} b'_0(0) + \underline{V}_{2,j-2} b'_1(0)] b_{-2}(v) \\
&+ [\underline{V}_{-1,j-1} b'_{-2}(0) + \underline{V}_{0,j-1} b'_{-1}(0) + \underline{V}_{1,j-1} b'_0(0) + \underline{V}_{2,j-1} b'_1(0)] b_{-1}(v) \\
&+ [\underline{V}_{-1,j} b'_{-2}(0) + \underline{V}_{0,j} b'_{-1}(0) + \underline{V}_{1,j} b'_0(0) + \underline{V}_{2,j} b'_1(0)] b_0(v) \\
&+ [\underline{V}_{-1,j+1} b'_{-2}(0) + \underline{V}_{0,j+1} b'_{-1}(0) + \underline{V}_{1,j+1} b'_0(0) + \underline{V}_{2,j+1} b'_1(0)] b_1(v) \\
&\qquad j = 1,2,\ldots,n \ ,
\end{aligned} \tag{3.33}$$

and

$$\begin{aligned}
\frac{\partial \underline{P}_{m,j}(u,v)}{\partial u}\Big|_{u=1} &= [\underline{V}_{m-2,j-2} b'_{-2}(1) + \underline{V}_{m-1,j-2} b'_{-1}(1) + \underline{V}_{m,j-2} b'_0(1) + \underline{V}_{m+1,j-2} b'_1(1)] b_{-2}(v) \\
&+ [\underline{V}_{m-2,j-1} b'_{-2}(1) + \underline{V}_{m-1,j-1} b'_{-1}(1) + \underline{V}_{m,j-1} b'_0(1) + \underline{V}_{m+1,j-1} b'_1(1)] b_{-1}(v) \\
&+ [\underline{V}_{m-2,j} b'_{-2}(1) + \underline{V}_{m-1,j} b'_{-1}(1) + \underline{V}_{m,j} b'_0(1) + \underline{V}_{m+1,j} b'_1(1)] b_0(v) \\
&+ [\underline{V}_{m-2,j+1} b'_{-2}(1) + \underline{V}_{m-1,j+1} b'_{-1}(1) + \underline{V}_{m,j+1} b'_0(1) + \underline{V}_{m+1,j+1} b'_1(1)] b_1(v) \\
&\qquad j = 1,2,\ldots,n \ .
\end{aligned} \tag{3.34}$$

Consulting Table 3.1 for the first parametric derivative

TABLE 3.1

First Parametric Derivative of the Subsectional Basis Functions

First Parametric Derivative	u=0	u=1
$b'_{-2}(u)=(-3u^2+6u-3)/6$	-1/2	0
$b'_{-1}(u)=(9u^2-12u)/6$	0	-1/2
$b'_{0}(u)=(-9u^2+6u+3)/6$	1/2	0
$b'_{1}(u)=3u^2/6$	0	1/2

values and substituting, yields

$$\frac{\partial \underline{P}_{-1,j}(u,v)}{\partial u}\Big|_{u=0} = \frac{1}{2}\Big\{[-\underline{V}_{-1,j-2} + \underline{V}_{1,j-2}]b_{-2}(v) + [-\underline{V}_{-1,j-1} + \underline{V}_{1,j-1}]b_{-1}(v) + [-\underline{V}_{-1,j} + \underline{V}_{1,j}]b_{0}(v) + [-\underline{V}_{-1,j+1} + \underline{V}_{1,j+1}]b_{1}(v)\Big\} \qquad (3.35)$$

$$j = 1,2,\ldots,n\ ,$$

and

$$\frac{\partial \underline{P}_{m,j}(u,v)}{\partial u}\Big|_{u=1} = \frac{1}{2}\Big\{[-\underline{V}_{m-1,j-2} + \underline{V}_{m+1,j-2}]b_{-2}(v) + [-\underline{V}_{m-1,j-1} + \underline{V}_{m+1,j-1}]b_{-1}(v) + [-\underline{V}_{m-1,j} + \underline{V}_{m+1,j}]b_{0}(v) + [-\underline{V}_{m-1,j+1} + \underline{V}_{m+1,j+1}]b_{1}(v)\Big\} \qquad (3.36)$$

$$j = 1,2,\ldots,n\ .$$

respectively. Substituting the constraints of (3.28) into

(3.35) and (3.36) gives

$$\left.\frac{\partial \underline{P}_{-1,j}(u,v)}{\partial u}\right|_{u=0} = \left\{\frac{1}{2}\left[-\underline{V}_{-m-1,j-2} + \underline{V}_{-1,j-2}\right]b_{-2}(v) + \left[-\underline{V}_{-m-1,j-1} + \underline{V}_{-1,j-1}\right]b_{-1}(v) + \left[-\underline{V}_{-m-1,j} + \underline{V}_{-1,j}\right]b_{0}(v) + \left[-\underline{V}_{-m-1,j+1} + \underline{V}_{-1,j+1}\right]b_{1}(v)\right\} \qquad (3.37)$$

$$j = 1,2,\ldots,n ,$$

and

$$\left.\frac{\partial \underline{P}_{m,j}(u,v)}{\partial u}\right|_{u=1} = \frac{1}{2}\left\{\left[-\underline{V}_{-m-1,j-2} + \underline{V}_{-1,j-2}\right]b_{-2}(v) + \left[-\underline{V}_{-m-1,j-1} + \underline{V}_{-1,j-1}\right]b_{-1}(v) + \left[-\underline{V}_{-m-1,j} + \underline{V}_{-1,j}\right]b_{0}(v) + \left[-\underline{V}_{-m-1,j+1} + \underline{V}_{-1,j+1}\right]b_{1}(v)\right\} \qquad (3.38)$$

$$j = 1,2,\ldots,n .$$

Therefore,

$$\left.\frac{\partial \underline{P}_{-1,j}(u,v)}{\partial u}\right|_{u=0} = \left.\frac{\partial \underline{P}_{m,j}(u,v)}{\partial u}\right|_{u=1} \qquad j = 1,2,\ldots,n . \qquad (3.39)$$

We can extend this principle to determine the second derivative along the same patch boundary. Differentiating (3.29) and (3.30) twice with respect to u and substituting the appropriate values for the second derivatives of the

TABLE 3.2

Second Parametric Derivative of the Subsectional Basis Functions

Second Parametric Derivative	u=0	u=1
$b''_{-2}(u)=(-6u+6)/6$	1	0
$b''_{-1}(u)=(18u-12)/6$	-2	1
$b''_{0}(u)=(-18u+6)/6$	1	-2
$b''_{1}(u)=6u/6$	0	1

subsectional basis functions (Table 3.2), results in

$$\frac{\partial^2 \underline{P}_{1,j}(u,v)}{\partial u^2}\Big|_{u=0} = [\underline{V}_{-1,j-2} - 2\underline{V}_{0,j-2} + \underline{V}_{1,j-2}]b_{-2}(v) + [\underline{V}_{-1,j-1} - 2\underline{V}_{0,j-1} + \underline{V}_{1,j-1}]b_{-1}(v) + [\underline{V}_{-1,j} - 2\underline{V}_{0,j} + \underline{V}_{1,j}]b_{0}(v) + [\underline{V}_{-1,j+1} - 2\underline{V}_{0,j+1} + \underline{V}_{1,j+1}]b_{1}(v) \qquad (3.40)$$

$$j = 1,2,\ldots,n ,$$

and

$$\frac{\partial^2 \underline{P}_{m,j}(u,v)}{\partial u^2}\Big|_{u=1} = [\underline{V}_{m-1,j-2} - 2\underline{V}_{m,j-2} + \underline{V}_{m+1,j-2}]b_{-2}(v) + [\underline{V}_{m-1,j-1} - 2\underline{V}_{m,j-1} + \underline{V}_{m+1,j-1}]b_{-1}(v) + [\underline{V}_{m-1,j} - 2\underline{V}_{m,j} + \underline{V}_{m+1,j}]b_{0}(v) + [\underline{V}_{m-1,j+1} - 2\underline{V}_{m,j+1} + \underline{V}_{m+1,j+1}]b_{1}(v) \qquad (3.41)$$

$$j = 1,2,\ldots,n .$$

Substitution of the control vertex constraints of (3.28)

into (3.40) and (3.41) yields

$$\left.\frac{\partial^2 \underline{P}_{1,j}(u,v)}{\partial u^2}\right|_{u=0} = [\underline{V}_{m-1,j-2} - 2\underline{V}_{m,j-2} + \underline{V}_{1,j-2}]b_{-2}(v) + [\underline{V}_{m-1,j-1} - 2\underline{V}_{m,j-1} + \underline{V}_{1,j-1}]b_{-1}(v)$$
$$+ [\underline{V}_{m-1,j} - 2\underline{V}_{m,j} + \underline{V}_{1,j}]b_0(v) + [\underline{V}_{m-1,j+1} - 2\underline{V}_{m,j+1} + \underline{V}_{1,j+1}]b_1(v) \qquad (3.42)$$
$$j = 1,2,\ldots,n ,$$

and

$$\left.\frac{\partial^2 \underline{P}_{m,j}(u,v)}{\partial u^2}\right|_{u=1} = [\underline{V}_{m-1,j-2} - 2\underline{V}_{m,j-2} + \underline{V}_{1,j-2}]b_{-2}(v) + [\underline{V}_{m-1,j-1} - 2\underline{V}_{m,j-1} + \underline{V}_{1,j-1}]b_{-1}(v)$$
$$+ [\underline{V}_{m-1,j} - 2\underline{V}_{m,j} + \underline{V}_{1,j}]b_0(v) + [\underline{V}_{m-1,j+1} - 2\underline{V}_{m,j+1} + \underline{V}_{1,j+1}]b_1(v) \qquad (3.43)$$
$$j = 1,2,\ldots,n .$$

Thus,

$$\left.\frac{\partial^2 \underline{P}_{1,j}(u,v)}{\partial u^2}\right|_{u=0} = \left.\frac{\partial^2 \underline{P}_{m,j}(u,v)}{\partial u^2}\right|_{u=1} \qquad j = 1,2,\ldots,n . \qquad (3.44)$$

In fact, a similar equality holds for the positional dependence (subject to the control vertex constraints) without the enforcement of the (n+1) patch-corner point constraints in (3.17).

$$\underline{P}_{1,j}(u,v)\Big|_{u=0} = \underline{P}_{m,j}(u,v)\Big|_{u=0} \qquad j = 1,2,\ldots,n . \qquad (3.45)$$

Thus, the following (n+1) patch-corner equations can be eliminated from (3.13):

$$\begin{aligned} \underline{P}_{0,0} &= \underline{P}_{1,j}(0,0) = \sum_{r=-2}^{1} \sum_{s=-2}^{1} \underline{V}_{1+r,j+s} b_r(0) b_s(0) \quad j = 1 , \\ \underline{P}_{0,j} &= \underline{P}_{1,j}(0,1) = \sum_{r=-2}^{1} \sum_{s=-2}^{1} \underline{V}_{1+r,j+s} b_r(0) b_s(1) \quad j = 1,2,\ldots,n . \end{aligned} \tag{3.46}$$

This leaves

$$\begin{aligned} \underline{P}_{i,j} &= \underline{P}_{i,j}(1,1) = \sum_{r=-2}^{1} \sum_{s=-2}^{1} \underline{V}_{i+r,j+s} b_r(1) b_s(1) \quad i = 1,2,\ldots,m \quad j = 1,2,\ldots,n , \\ \underline{P}_{i,j-1} &= \underline{P}_{i,j}(1,0) = \sum_{r=-2}^{1} \sum_{s=-2}^{1} \underline{V}_{i+r,j+s} b_r(1) b_s(0) \quad i = 1,2,\ldots,m \quad j = 1 . \end{aligned} \tag{3.47}$$

as the (m)(n+1) distinct patch-corner equations.

Therefore, the effect of the 3(n+3) control vertex constraints in (3.28) on the closed surface formulation is twofold. Firstly, it ensures positional, first derivative, and second derivative continuity in the parametric u-direction along the patch merger. Secondly, it reduces the number of patch-corner equations from (m+1)(n+1) to (m)(n+1) while introducing an additional 3(n+3) equations by way of vertex constraints. The outcome is an augmented system comprised of (m)(n+1)+3(n+3) equations in (m+3)(n+3) unknown control vertices.

3.2.2.2 Continuity at the v-Parameter Extremes

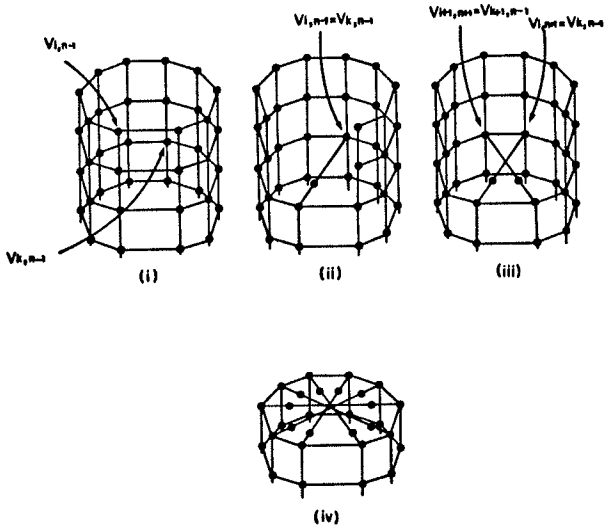

Figure 3.9: Overlapping the diagonal control vertices.

To demonstrate that positional, first derivative, and second derivative continuity can be preserved at the v-parameter extremes by manipulating the control vertex structure, consider the cylinder-like orientation of control vertices in Figure 3.9. It was demonstrated that derivative continuity is secured in the u-direction by overlapping the boundary control vertices. This same technique can be applied to the control vertices bordering the v extremes.

To illustrate this feature, consider the control vertices

$$\begin{matrix} \underline{V}_{i,n+1} \\ \underline{V}_{i,-1} \end{matrix} \quad , \quad i = 1,2,\ldots,m \; . \tag{3.48}$$

which traverse the top-most and bottom-most levels of the control mesh (Figure 3.9). Notice that the constraint in (3.28) is taken into consideration, thereby restricting the notation to the distinct control vertices. To exploit the merits of overlapping control vertices, let each top-most control vertex be equated to its diagonal counterpart two levels down (Figure 3.9). Likewise, let the bottom control vertices be similarly arranged, thereby, introducing (2m) additional constraints, given by

$$\begin{matrix} \underline{V}_{i,n+1} = \underline{V}_{k,n-1} \\ \underline{V}_{i,-1} = \underline{V}_{k,1} \end{matrix} \quad i = 1,2,\ldots,m \quad k = \begin{cases} i + \frac{m}{2} & i \leq \frac{m}{2} \\ i - \frac{m}{2} & i > \frac{m}{2} \end{cases} . \tag{3.49}$$

To achieve diagonal correspondence between control vertices, there must be a one-to-one relationship between overlapped vertices. As a result, (m) must be even. Moreover, the number of patches in the parametric u-direction must be even when modelling closed surfaces.

Before addressing the matter of diagonal surface patch continuity at these parametric extremes, recall that positional continuity is guaranteed by the enforcement of

$$\begin{aligned} \underline{P}_{1,0} &= \underline{P}_{2,0} = \cdots = \underline{P}_{m-1,0} = \underline{P}_{m,0} \\ \underline{P}_{1,n} &= \underline{P}_{2,n} = \cdots = \underline{P}_{m-1,n} = \underline{P}_{m,n} \end{aligned} \tag{3.50}$$

This equality of patch-corner points, together with the (2m) control vertex constraints in (3.49), results in additional control vertex information which is essential in demonstrating continuity between diagonal patches at these points. We will restrict our attention to the control vertices which support the top-most surface patches, and point out that similar results hold for the control vertices which influence the bottom-most surface patches.

Equation (3.50) and the manner in which the surface patches are oriented require that

$$\underline{P}_{i,n} = \underline{P}_{i,n}(u,v)\Big|_{u=1,v=1} \quad , \quad \underline{P}_{k,n} = \underline{P}_{k,n}(u,v)\Big|_{u=1,v=1} \quad . \tag{3.51}$$

Hence,

$$\underline{P}_{i,n}(u,v)\Big|_{u=1,v=1} = \underline{P}_{k,n}(u,v)\Big|_{u=1,v=1} \qquad i = 1,2,\ldots,\frac{m}{2} . \tag{3.52}$$

Expanding the left- and right-hand sides of (3.52) gives

$$\begin{aligned} \underline{P}_{i,n} &= \underline{P}_{i,n}(1,1) = \sum_{r=-2}^{1} \sum_{s=-2}^{1} \underline{V}_{i+r,n+s} b_r(1) b_s(1) , \\ &= [\underline{V}_{i-1,n-1} + 4\underline{V}_{i,n-1} + \underline{V}_{i+1,n-1} + 4\underline{V}_{i-1,n} + 16\underline{V}_{i,n} + 4\underline{V}_{i+1,n} + \underline{V}_{i-1,n+1} + 4\underline{V}_{i,n+1} + \underline{V}_{i+1,n+1}]/36 \\ &\qquad i = 1,2,\ldots,\tfrac{m}{2} , \end{aligned} \tag{3.53}$$

and

$$\begin{aligned} \underline{P}_{k,n} &= \underline{P}_{k,n}(1,1) = \sum_{r=-2}^{1} \sum_{s=-2}^{1} \underline{V}_{k+r,n+s} b_r(1) b_s(1) , \\ &= [\underline{V}_{k-1,n-1} + 4\underline{V}_{k,n-1} + \underline{V}_{k+1,n-1} + 4\underline{V}_{k-1,n} + 16\underline{V}_{k,n} + 4\underline{V}_{k+1,n} + \underline{V}_{k-1,n+1} + 4\underline{V}_{k,n+1} + \underline{V}_{k+1,n+1}]/36 \\ &\qquad k = i + \tfrac{m}{2} . \end{aligned} \tag{3.54}$$

Applying the control vertex constraints of (3.49) yields

$$\begin{aligned} \underline{P}_{i,n} = [&\underline{V}_{i-1,n-1} + 4\underline{V}_{i,n-1} + \underline{V}_{i+1,n-1} + 4\underline{V}_{i-1,n} + 16\underline{V}_{i,n} \\ &+ 4\underline{V}_{i+1,n} + \underline{V}_{k-1,n-1} + 4\underline{V}_{k,n-1} + \underline{V}_{k+1,n-1}]/36 , \end{aligned} \tag{3.55}$$

and

$$\underline{P}_{k,n} = [\underline{V}_{k-1,n-1} + 4\underline{V}_{k,n-1} + \underline{V}_{k+1,n-1} + 4\underline{V}_{k-1,n} + 16\underline{V}_{k,n} + 4\underline{V}_{k+1,n} + \underline{V}_{i-1,n-1} + 4\underline{V}_{i,n-1} + \underline{V}_{i+1,n-1}]/36 \ . \tag{3.56}$$

Subtracting (3.56) from (3.57) results in

$$\underline{P}_{i,n} - \underline{P}_{k,n} = [\underline{V}_{i-1,n} - \underline{V}_{k-1,n} + 4\underline{V}_{i,n} - 4\underline{V}_{k,n} + \underline{V}_{i+1,n} - \underline{V}_{k+1,n}] \ . \tag{3.57}$$

Moreover, m/2 linear independent equations can be generated as follows:

$$\begin{aligned}
\underline{P}_{1,n} - \underline{P}_{\frac{m}{2}+1,n} &= [\underline{V}_{m,n} - \underline{V}_{\frac{m}{2},n} + 4\underline{V}_{1,n} - 4\underline{V}_{\frac{m}{2}+1,n} + \underline{V}_{2,n} - \underline{V}_{\frac{m}{2}+2,n}]/4 \ , \\
&\vdots \qquad\qquad\qquad\qquad \vdots \\
\underline{P}_{i,n} - \underline{P}_{k,n} &= [\underline{V}_{i-1,n} - \underline{V}_{k-1,n} + 4\underline{V}_{i,n} - 4\underline{V}_{k,n} + \underline{V}_{i+1,n} - \underline{V}_{k+1,n}]/4 \ , \\
&\vdots \qquad\qquad\qquad\qquad \vdots \\
\underline{P}_{\frac{m}{2},n} - \underline{P}_{m,n} &= [\underline{V}_{\frac{m}{2}-1,n} - \underline{V}_{m-1,n} + 4\underline{V}_{\frac{m}{2},n} - 4\underline{V}_{m,n} + \underline{V}_{\frac{m}{2}+1,n} - \underline{V}_{1,n}]/4 \ .
\end{aligned} \tag{3.58}$$

Letting

$$\begin{aligned}
\underline{V}_{1,n} - \underline{V}_{\frac{m}{2}+1,n} &= \alpha_1 \ , \\
&\vdots \qquad\qquad \vdots \\
\underline{V}_{i,n} - \underline{V}_{k,n} &= \alpha_i \ , \\
&\vdots \qquad\qquad \vdots \\
\underline{V}_{\frac{m}{2},n} - \underline{V}_{m,n} &= \alpha_{\frac{m}{2}} \ .
\end{aligned} \tag{3.59}$$

(3.58) can be rewritten, yielding

$$\begin{aligned}
P_{1,n} - P_{\frac{m}{2}+1,n} &= -\alpha_{\frac{m}{2}} + 4\alpha_1 + \alpha_2 \,, \\
&\vdots \qquad\qquad\qquad\quad \vdots \\
P_{i,n} - P_{k,n} &= \alpha_{i-1} + 4\alpha_i + \alpha_{i+1} \,, \\
&\vdots \qquad\qquad\qquad\quad \vdots \\
P_{\frac{m}{2},n} - P_{m,n} &= \alpha_{\frac{m}{2}-1} + 4\alpha_{\frac{m}{2}} - \alpha_1 \,.
\end{aligned} \tag{3.60}$$

However, from the corner point constraints in (3.50), it is evident that

$$\begin{aligned}
P_{1,n} - P_{\frac{m}{2}+1,n} &= 0 \,, \\
&\vdots \\
P_{i,n} - P_{k,n} &= 0 \,, \\
&\vdots \\
P_{\frac{m}{2},n} - P_{m,n} &= 0 \,.
\end{aligned} \tag{3.61}$$

Thus, m/2 homogeneous equations in m/2 unknowns results:

$$\begin{bmatrix}
4 & 1 & & & & -1 \\
1 & 4 & 1 & & & \\
 & \ddots & \ddots & \ddots & & \\
 & & 1 & 4 & 1 & \\
-1 & & & 1 & 4 &
\end{bmatrix}
\begin{bmatrix}
\alpha_1 \\ \alpha_2 \\ \vdots \\ \alpha_{\frac{m}{2}-1} \\ \alpha_{\frac{m}{2}}
\end{bmatrix} = [0] \,. \tag{3.62}$$

Since the determinant is never zero, the only possible

(deterministic) solution is

$$\alpha_1 = \alpha_2 = \ldots = \alpha_i = \ldots = \alpha_{\frac{m}{2}-1} = \alpha_{\frac{m}{2}} = 0 \, . \tag{3.63}$$

Moreover, back substitution into (3.59) gives

$$\begin{aligned} \underline{V}_{1,n} &= \underline{V}_{\frac{m}{2}+1,n} \, , \\ &\vdots \\ \underline{V}_{i,n} &= \underline{V}_{k,n} \, , \\ &\vdots \\ \underline{V}_{\frac{m}{2},n} &= \underline{V}_{m,n} \, . \end{aligned} \tag{3.64}$$

In fact, the same result holds for

$$\begin{aligned} \underline{V}_{1,0} &= \underline{V}_{\frac{m}{2}+1,0} \, , \\ &\vdots \\ \underline{V}_{i,0} &= \underline{V}_{k,0} \, , \\ &\vdots \\ \underline{V}_{\frac{m}{2},0} &= \underline{V}_{m,0} \, . \end{aligned} \tag{3.65}$$

Therefore, equating patch-corner points at the v-parameter extremes, along with the vertex constraints in (3.18) and (3.19), results in an equality of diagonal control vertices about the control mesh at j=n and j=0.

The results in (3.64) and (3.65) are not imposed constraints, they are merely the consequence of the patch-corner constraints in (3.50). However, it is

conceivable that the equality of diagonal control vertices in (3.64) and (3.65) could have been enforced at the outset, thereby always yielding

$$\underline{P}_{i,n} = \underline{P}_{k,n} \ , \ \underline{P}_{i,0} = \underline{P}_{k,0} \quad i = 1,2,\ldots,\frac{m}{2} \ . \tag{3.66}$$

However, this would restrict the formulation to the description of closed surfaces and would not lend itself to the specification of quasi-closed bicubic surfaces, to be addressed in ensuing sections.

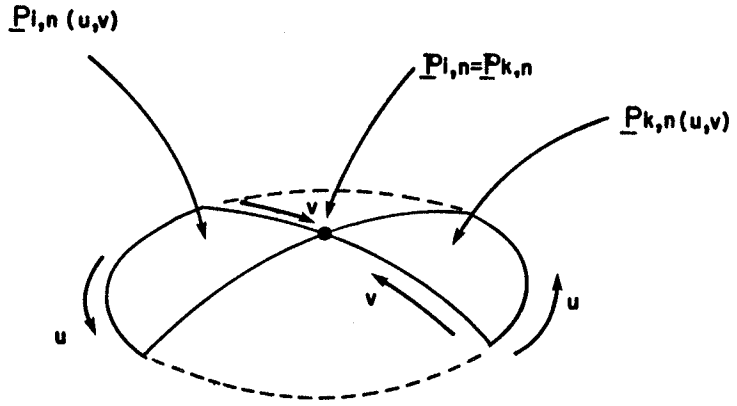

Figure 3.10: Two diagonal corresponding surface patches.

To show that first derivative and second derivative continuity is preserved between diagonal surface patches,

consider the two patches in Figure 3.10, given by

$$\underline{P}_{i,n}(u,v) = \sum_{r=-2}^{1} \sum_{s=-2}^{1} \underline{V}_{i+r,n+s} b_r(u) b_s(v) \quad i = 1,2,\ldots,\frac{m}{2}, \tag{3.67}$$

and

$$\underline{P}_{k,n}(u,v) = \sum_{r=-2}^{1} \sum_{s=-2}^{1} \underline{V}_{k+r,n+s} b_r(u) b_s(v) \quad k = i + \frac{m}{2} . \tag{3.68}$$

For first derivative and second derivative continuity, the following must hold:

$$\left.\frac{\partial \underline{P}_{i,n}(u,v)}{\partial v}\right|_{v=1} = \left.\frac{\partial \underline{P}_{k,n}(u,v)}{\partial(-v)}\right|_{v=1} \quad i = 1,2,\ldots,\frac{m}{2} \quad k = i + \frac{m}{2} , \tag{3.69}$$

and

$$\left.\frac{\partial^2 \underline{P}_{i,n}(u,v)}{\partial v^2}\right|_{v=1} = \left.\frac{\partial^2 \underline{P}_{k,n}(u,v)}{\partial(-v)^2}\right|_{v=1} \quad i = 1,2,\ldots,\frac{m}{2} \quad k = i + \frac{m}{2} . \tag{3.70}$$

The (-v) is included to compensate for the opposing parametric v orientations of each surface patch. Expanding

the left-hand side of (3.69) yields

$$\left.\frac{\partial \underline{P}_{i,n}(u,v)}{\partial v}\right|_{v=1} = [\underline{V}_{i-2,n-2}b_{-2}(u) + \underline{V}_{i-1,n-2}b_{-1}(u) + \underline{V}_{i,n-2}b_0(u) + \underline{V}_{i+1,n-2}b_1(u)]b'_{-2}(1)$$
$$+ [\underline{V}_{i-2,n-1}b_{-2}(u) + \underline{V}_{i-1,n-1}b_{-1}(u) + \underline{V}_{i,n-1}b_0(u) + \underline{V}_{i+1,n-1}b_1(u)]b'_{-1}(1)$$
$$+ [\underline{V}_{i-2,n}b_{-2}(u) + \underline{V}_{i-1,n}b_{-1}(u) + \underline{V}_{i,n}b_0(u) + \underline{V}_{i+1,n}b_1(u)]b'_0(1)$$
$$+ [\underline{V}_{i-2,n+1}b_{-2}(u) + \underline{V}_{i-1,n+1}b_{-1}(u) + \underline{V}_{i,n+1}b_0(u) + \underline{V}_{i+1,n+1}b_1(u)]b'_1(1) . \qquad (3.71)$$

Similarly, for the right-hand side

$$\left.\frac{\partial \underline{P}_{k,n}(u,v)}{\partial(-v)}\right|_{v=1} = -[\underline{V}_{k-2,n-2}b_{-2}(u) + \underline{V}_{k-1,n-2}b_{-1}(u) + \underline{V}_{k,n-2}b_0(u) + \underline{V}_{k+1,n-2}b_1(u)]b'_{-2}(1)$$
$$- [\underline{V}_{k-2,n-1}b_{-2}(u) + \underline{V}_{k-1,n-1}b_{-1}(u) + \underline{V}_{k,n-1}b_0(u) + \underline{V}_{k+1,n-1}b_1(u)]b'_{-1}(1)$$
$$- [\underline{V}_{k-2,n}b_{-2}(u) + \underline{V}_{k-1,n}b_{-1}(u) + \underline{V}_{k,n}b_0(u) + \underline{V}_{k+1,n}b_1(u)]b'_0(1)$$
$$- [\underline{V}_{k-2,n+1}b_{-2}(u) + \underline{V}_{k-1,n+1}b_{-1}(u) + \underline{V}_{k,n+1}b_0(u) + \underline{V}_{k+1,n+1}b_1(u)]b'_1(1) . \qquad (3.72)$$

Substituting the subsectional basis function values from Table 3.1 at v=1, (3.71) and (3.72) become

$$\left.\frac{\partial \underline{P}_{i,n}(u,v)}{\partial v}\right|_{v=1} = \tfrac{1}{2}[-\underline{V}_{i-2,n-1}b_{-2}(u) - \underline{V}_{i-1,n-1}b_{-1}(u) - \underline{V}_{i,n-1}b_0(u) - \underline{V}_{i+1,n-1}b_1(u)]$$
$$+ \tfrac{1}{2}[\underline{V}_{i-2,n+1}b_{-2}(u) + \underline{V}_{i-1,n+1}b_{-1}(u) + \underline{V}_{i,n+1}b_0(u) + \underline{V}_{i+1,n+1}b_1(u)] \qquad (3.73)$$

and

$$\left.\frac{\partial \underline{P}_{k,n}(u,v)}{\partial(-v)}\right|_{v=1} = -\tfrac{1}{2}[-\underline{V}_{k-2,n-1}b_{-2}(u) - \underline{V}_{k-1,n-1}b_{-1}(u) - \underline{V}_{k,n-1}b_0(u) - \underline{V}_{k+1,n-1}b_1(u)]$$
$$- \tfrac{1}{2}[\underline{V}_{k-2,n+1}b_{-2}(u) + \underline{V}_{k-1,n+1}b_{-1}(u) + \underline{V}_{k,n+1}b_0(u) + \underline{V}_{k+1,n+1}b_1(u)] . \qquad (3.74)$$

Applying the control vertex constraints in (3.49) gives

$$\left.\frac{\partial \underline{P}_{i,n}(u,v)}{\partial v}\right|_{v=1} = \tfrac{1}{2}[-\underline{V}_{i-2,n-1}b_{-2}(u) - \underline{V}_{i-1,n-1}b_{-1}(u) - \underline{V}_{i,n-1}b_0(u) - \underline{V}_{i+1,n-1}b_1(u)] + \tfrac{1}{2}[\underline{V}_{k-2,n-1}b_{-2}(u) + \underline{V}_{k-1,n-1}b_{-1}(u) + \underline{V}_{k,n-1}b_0(u) - \underline{V}_{k+1,n-1}b_1(u)] , \tag{3.75}$$

and

$$\left.\frac{\partial \underline{P}_{k,n}(u,v)}{\partial(-v)}\right|_{v=1} = \tfrac{1}{2}[\underline{V}_{k-2,n-1}b_{-2}(u) + \underline{V}_{k-1,n-1}b_{-1}(u) + \underline{V}_{k,n-1}b_0(u) + \underline{V}_{k+1,n-1}b_1(u)] + \tfrac{1}{2}[-\underline{V}_{i-2,n-1}b_{-2}(u) - \underline{V}_{i-1,n-1}b_{-1}(u) - \underline{V}_{i,n-1}b_0(u) - \underline{V}_{i+1,n-1}b_1(u)] . \tag{3.76}$$

Clearly, the first derivative is continuous:

$$\left.\frac{\partial \underline{P}_{i,n}(u,v)}{\partial v}\right|_{v=1} = \left.\frac{\partial \underline{P}_{k,n}(u,v)}{\partial(-v)}\right|_{v=1} \qquad i = 1,2,\ldots,\frac{m}{2} \quad k = i + \frac{m}{2} , \tag{3.77}$$

For second derivative continuity (3.70) must hold. Expanding the left- and right-hand sides, and substituting the values of second derivative of the subsectional basis functions at v=1 yields

$$\left.\frac{\partial^2 \underline{P}_{i,n}(u,v)}{\partial v^2}\right|_{v=1} = [\underline{V}_{i-2,n-1}b_{-2}(u) + \underline{V}_{i-1,n-1}b_{-1}(u) + \underline{V}_{i,n-1}b_0(u) + \underline{V}_{i+1,n-1}b_1(u)] - 2[\underline{V}_{i-2,n}b_{-2}(u) + \underline{V}_{i-1,n}b_{-1}(u) + \underline{V}_{i,n}b_0(u) + \underline{V}_{i+1,n}b_1(u)] + [\underline{V}_{i-2,n+1}b_{-2}(u) + \underline{V}_{i-1,n+1}b_{-1}(u) + \underline{V}_{i,n+1}b_0(u) + \underline{V}_{i+1,n+1}b_1(u)] , \tag{3.78}$$

and

$$\frac{\partial^2 \underline{P}_{k,n}(u,v)}{\partial(-v)^2}\Big|_{v=1} = [\underline{V}_{k-2,n-1}b_{-2}(u) + \underline{V}_{k-1,n-1}b_{-1}(u) + \underline{V}_{k,n-1}b_0(u) + \underline{V}_{k+1,n-1}b_1(u)]$$
$$- 2[\underline{V}_{k-2,n}b_{-2}(u) + \underline{V}_{k-1,n}b_{-1}(u) + \underline{V}_{k,n}b_0(u) + \underline{V}_{k+1,n}b_1(u)] \qquad (3.79)$$
$$+ [\underline{V}_{k-2,n+1}b_{-2}(u) + \underline{V}_{k-1,n+1}b_{-1}(u) + \underline{V}_{k,n+1}b_0(u) + \underline{V}_{k+1,n+1}b_1(u)] ,$$

Applying the constraints in (3.49), gives

$$\frac{\partial^2 \underline{P}_{i,n}(u,v)}{\partial v^2}\Big|_{v=1} = [\underline{V}_{i-2,n-1}b_{-2}(u) + \underline{V}_{i-1,n-1}b_{-1}(u) + \underline{V}_{i,n-1}b_0(u) + \underline{V}_{i+1,n+1}b_1(u)]$$
$$- 2[\underline{V}_{i-2,n}b_{-2}(u) + \underline{V}_{i-1,n}b_{-1}(u) + \underline{V}_{i,n}b_0(u) + \underline{V}_{i+1,n}b_1(u)] \qquad (3.80)$$
$$+ [\underline{V}_{k-2,n-1}b_{-2}(u) + \underline{V}_{k-1,n-1}b_{-1}(u) + \underline{V}_{k,n-1}b_0(u) + \underline{V}_{k+1,n-1}b_1(u)] .$$

and

$$\frac{\partial^2 \underline{P}_{k,n}(u,v)}{\partial(-v)^2}\Big|_{v=1} = [\underline{V}_{k-2,n-1}b_{-2}(u) + \underline{V}_{k-1,n-1}b_{-1}(u) + \underline{V}_{k,n-1}b_0(u) + \underline{V}_{k+1,n-1}b_1(u)]$$
$$- 2[\underline{V}_{k-2,n}b_{-2}(u) + \underline{V}_{k-1,n}b_{-1}(u) + \underline{V}_{k,n}b_0(u) + \underline{V}_{k+1,n}b_1(u)] \qquad (3.81)$$
$$+ [\underline{V}_{i-2,n-1}b_{-2}(u) + \underline{V}_{i-1,n-1}b_{-1}(u) + \underline{V}_{i,n-1}b_0(u) + \underline{V}_{i+1,n-1}b_1(u)] .$$

It is clear that the following must hold for second derivative continuity:

$$[\underline{V}_{i-2,n}b_{-2}(u) + \underline{V}_{i-2,n}b_{-1}(u) + \underline{V}_{i,n}b_0(u) + \underline{V}_{i+1,n}b_1(u)] \qquad (3.82)$$
$$= [\underline{V}_{k-2,n}b_{-2}(u) + \underline{V}_{k-1,n}b_{-1}(u) + \underline{V}_{k,n}b_0(u) + \underline{V}_{k+1,n}b_1(u)] .$$

Recall that enforcing equality of patch corners, subject to the (2m) control vertex constraints of (3.49), results in

$$\begin{aligned} \underline{V}_{i,0} &= \underline{V}_{k,0} \quad i = 1,2,\ldots,\frac{m}{2} \quad k = i + \frac{m}{2} , \\ \underline{V}_{i,n} &= \underline{V}_{k,n} \quad i = 1,2,\ldots,\frac{m}{2} \quad k = i + \frac{m}{2} . \end{aligned} \tag{3.83}$$

Thus, the result in (3.82) holds and there is second derivative continuity between diagonal surface patches. Identical results exist between the bottom-most diagonal patches of the closed surface:

$$\frac{\partial \underline{P}_{i,0}(u,v)}{\partial v}\bigg|_{v=0} = \frac{\partial \underline{P}_{k,0}(u,v)}{\partial(-v)}\bigg|_{v=0} \quad i = 1,2,\ldots,\frac{m}{2} \quad k = i + \frac{m}{2} , \tag{3.84}$$

$$\frac{\partial^2 \underline{P}_{i,0}(u,v)}{\partial v^2}\bigg|_{v=0} = \frac{\partial^2 \underline{P}_{k,0}(u,v)}{\partial(-v)^2}\bigg|_{v=0} \quad i = 1,2,\ldots,\frac{m}{2} \quad k = i + \frac{m}{2} . \tag{3.85}$$

By manipulating the control vertex structure into a specified closed form, the necessity of prescribing first derivative and second derivative boundary constraints between merged patch borders can be avoided; yet, positional, first derivative, and second derivative continuity is inherently guaranteed everywhere on the closed surface. Moreover, the enforcement of control vertex

constraints in (3.28) and (3.49) introduces 3(n+3) and (2m) constraint equations respectively. These, combined with the (m)(n+1) patch-corner equations, yield a determinable system of

$$(m)(n + 1) + 3(n + 3) + (2m) = (m + 3)(n + 3) \qquad (3.86)$$

equations in (m+3)(n+3) unknown control vertices.

3.2.3 Quasi-Closed Surface Representation

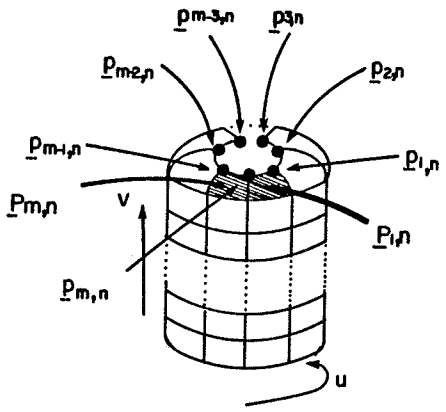

Figure 3.11: Quasi-closed surface patch arrangement.

The quasi-closed bicubic surface formulation is mathematically equivalent to that of the closed bicubic surface. It is characterized by having an open surface patch structure at either one or both of the v-parameter extremes (Figure 3.11). The quasi-closed formulation has a closed control vertex structure identical to that of the closed formulation, hence, the term quasi-closed.

In the preceding discussion on the closed surface patch arrangement, a closed surface was obtained by first merging the u-parameter extremes of an open patch structure. Secondly, to achieve closure at the v-parameter extremes, the patch-corner equations given by

$$\underline{P}_{i,0} = \underline{P}_{i,1}^{(u,v)}\Big|_{u=1,v=0} = \sum_{r=-2}^{1} \sum_{s=-2}^{1} \underline{V}_{i+r,1+s} b_r(1) b_s(0) \quad i = 1,2,\ldots,m \,, \tag{3.87}$$

and

$$\underline{P}_{i,n} = \underline{P}_{i,n}^{(u,v)}\Big|_{u=1,v=1} = \sum_{r=-2}^{1} \sum_{s=-2}^{1} \underline{V}_{i+r,n+s} b_r(1) b_s(1) \quad i = 1,2,\ldots,m \,, \tag{3.88}$$

were forced to coalesce to a single point. That is

$$\begin{aligned} \underline{P}_{1,0} &= \underline{P}_{2,0} = \cdots = \underline{P}_{m-1,0} = \underline{P}_{m,0} \\ \underline{P}_{1,n} &= \underline{P}_{2,n} = \cdots = \underline{P}_{m-1,n} = \underline{P}_{m,n} \end{aligned} \tag{3.89}$$

This equality of patch-corner points was essential to attain complete closure of the surface and hence, continuity.

The equations in (3.87) and (3.88) constitute (2m) of the (m)(n+1) patch-corner equations of the closed formulation. If the restriction of equality of patch-corner points is removed at either one or both of the v-parameter extremes, thereby allowing the patch-corner equations to interpolate

(m) distinct points, the patch-corner equation structure remains unchanged. Only the point to which it is equated to is altered. As a result, there are still (m)(n+1) patch-corner equations interpolating:

1. (m)(n+1) distinct points in the case of a quasi-closed surface opened at both extremes, and
2. (m)(n)+1 distinct points in the case of one open v extreme.

3.2.3.1 Surface Edge Artifact

The control vertex structure used to support the quasi-closed surface is identical to that used with closed bicubic surfaces. Supporting m by n surface patches arranged in a quasi-closed form requires (m+3)(n+3) control vertices. These vertices are restricted by the control vertex constraints. That is

$$\begin{aligned} \underline{V}_{0,j} &= \underline{V}_{m,j} \,, \\ \underline{V}_{-1,j} &= \underline{V}_{m-1,j} \,, \quad j = -1,0,1,\ldots,n,n+1 \,, \\ \underline{V}_{m+1,j} &= \underline{V}_{1,j} \,, \end{aligned} \tag{3.90}$$

and

$$\begin{aligned} \underline{V}_{i,n+1} &= \underline{V}_{k,n-1} \\ \underline{V}_{i,-1} &= \underline{V}_{k,1} \end{aligned} \qquad i = 1,2,\ldots,m \quad k = \begin{Bmatrix} i + \frac{m}{2} & i \le \frac{m}{2} \\ i - \frac{m}{2} & i > \frac{m}{2} \end{Bmatrix}. \tag{3.91}$$

The ramifications of the first constraint are as in the closed surface formulation, a guarantee of positional, first derivative and second derivative continuity in the u-direction along the patch merger. The second set of constraints, on the otherhand, influences quasi-closed surfaces in a different manner than that of closed surfaces.

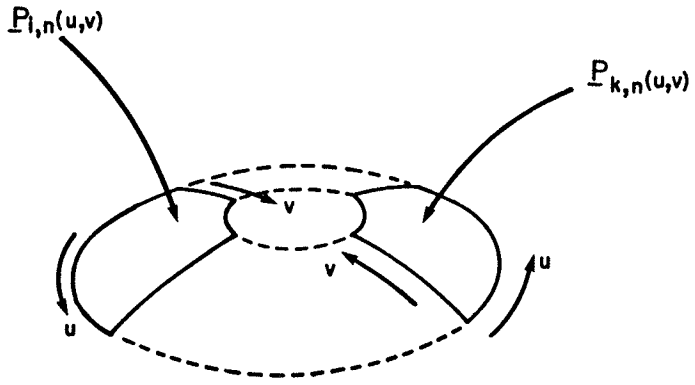

Figure 3.12: Two diagonal patches of a quasi-closed surface.

Consider two diagonal corresponding surface patches illustrated in Figure 3.12. The surface patch equations are given by

$$\underline{P}_{i,n}(u,v) = \sum_{r=-2}^{1} \sum_{s=-2}^{1} \underline{V}_{i+r,n+s} b_r(u) b_s(v) \quad i = 1,2,\ldots,\frac{m}{2}, \quad (3.92)$$

and

$$\underline{P}_{k,n}(u,v) = \sum_{r=-2}^{1} \sum_{s=-2}^{1} \underline{V}_{k+r,n+s} b_r(u) b_s(v) \qquad k = i + \frac{m}{2} \quad . (3.93)$$

Subject to the constraints in (3.91), the first derivative with respect to v for $\underline{P}_{i,n}$ agrees with the first derivative with respect to (-v) of $\underline{P}_{k,n}$ at the same parametric location despite being remote from each other in R^3. That is

$$\left.\frac{\partial \underline{P}_{i,n}(u,v)}{\partial v}\right|_{v=1} = \left.\frac{\partial \underline{P}_{k,n}(u,v)}{\partial(-v)}\right|_{v=1} \qquad i = 1,2,\ldots,\frac{m}{2} \quad k = i + \frac{m}{2} \quad , (3.94)$$

However, the same cannot be said for the second derivative. This can been attributed to one feature that distinguishes the quasi-closed formulation from the closed formulation: the removal of the patch-corner constraints in (3.89), which allows for the specification of quasi-closed surfaces. Recall that with the patch-corner point constraints in place, the following results:

$$\begin{aligned} \underline{V}_{i,0} &= \underline{V}_{k,0} \qquad i = 1,2,\ldots,\frac{m}{2} \quad k = i + \frac{m}{2} \quad , \\ \underline{V}_{i,n} &= \underline{V}_{k,n} \qquad i = 1,2,\ldots,\frac{m}{2} \quad k = i + \frac{m}{2} \quad . \end{aligned} \qquad (3.95)$$

This additional information, in conjunction with the constraints in (3.91), permits the continuity of the second

derivative (See (3.70)). In the quasi-closed surface formulation, where either one or both of the v-parameter extremes are opened, the identities in (3.95) are invalid since they are contingent upon the enforcement of the patch-corner point constraints. Thus, for quasi-closed surfaces, the second derivative with respect to v does not necessarily emulate its diagonal counterpart.

The first derivative in (3.94), which can be viewed as the surface tangent vector, imitates the edge tangent of its diagonal counterpart and, as a result, introduces surface-edge artifacts. This behavior at the open surface edges is primarily due to the underlying closed control vertex structure. The surface is being constrained to interpolate distinct points at one or both of the v-parameter extremes, while concurrently accommodating the influence of the control vertex structure. When the combined effect of these two constraints becomes too great, it manifests itself as an unexpected edge overshoot.

Although the closed and quasi-closed formulations exhibit distinctive surface properties, they are based on an identical system of equations. Hence, a unified matrix structure, comprised of patch-corner equations and control vertex constraints, has the flexibility to cater to both closed and quasi-closed surface representations.

In the following section , the formation of the control vertex matrix and its application to closed and quasi-closed surfaces is presented.

3.2.4 Control Vertex Matrix Structure

In order to interpolate a closed or quasi-closed network of points with bicubic B-spline surface patches, the control vertices which support the surface must be uniquely determined. For both closed and quasi-closed surface interpolation, the control vertex matrix structures are identical.

Consider m by n surface patches interpolating either a closed or quasi-closed network of points in R^3. This surface patch arrangement requires the support of (m+3)(n+3) unknown control vertices. Clearly, to obtain a determinable system, (m+3)(n+3) equations are required. The (m)(n+1) patch-corner equations are given by

$$P_{i,j} = \underline{P}_{i,j}(1,1) = \sum_{r=-2}^{1} \sum_{s=-2}^{1} \underline{V}_{i+r,j+s} b_r(1) b_s(1) \quad i = 1,2,\ldots,m \quad j = 1,2,\ldots,n , \tag{3.96}$$

and

$$P_{i,j-1} = \underline{P}_{i,j}(1,0) = \sum_{r=-2}^{1} \sum_{s=-2}^{1} \underline{V}_{i+r,j+s} b_r(1) b_s(0) \quad i = 1,2,\ldots,m \quad j = 1 . \tag{3.97}$$

The control vertex constraints contribute 3(n+3)+(2m)

equations, given by

$$\begin{aligned} \underline{V}_{0,j} &= \underline{V}_{m,j} \ , \\ \underline{V}_{-1,j} &= \underline{V}_{m-1,j} \ , \quad j = -1,0,1,\ldots,n,n+1 \ , \\ \underline{V}_{m+1,j} &= \underline{V}_{1,j} \ , \end{aligned} \tag{3.98}$$

and

$$\begin{aligned} \underline{V}_{i,n+1} &= \underline{V}_{k,n-1} \\ \underline{V}_{i,-1} &= \underline{V}_{k,1} \end{aligned} \qquad i = 1,2,\ldots,m \quad k = \begin{Bmatrix} i + \frac{m}{2} & i \le \frac{m}{2} \\ i - \frac{m}{2} & i > \frac{m}{2} \end{Bmatrix}. \tag{3.99}$$

Thus, equations (3.96) through (3.99), generate (m+3)(n+3) equations in (m+3)(n+3) unknown control vertices.

There is a choice of two methodologies to follow in accumulating the system matrix:

1. combine the (m+3)(n+3) equations into a matrix of dimension (m+3)(n+3), or
2. combine the (m)(n+1) patch-corner equations, subject to the control vertex constraints, thereby constructing a reduced system matrix of (m)(n+1) equations in (m)(n+1) <u>distinct</u> control vertices.

Implementing the latter of these has the advantage of requiring less computational effort due to the compressed matrix size. In this instance, once the distinct control vertices have been determined, the complete set of (m+3)(n+3) control vertices is ascertained by a reverse application of the control vertex constraints.

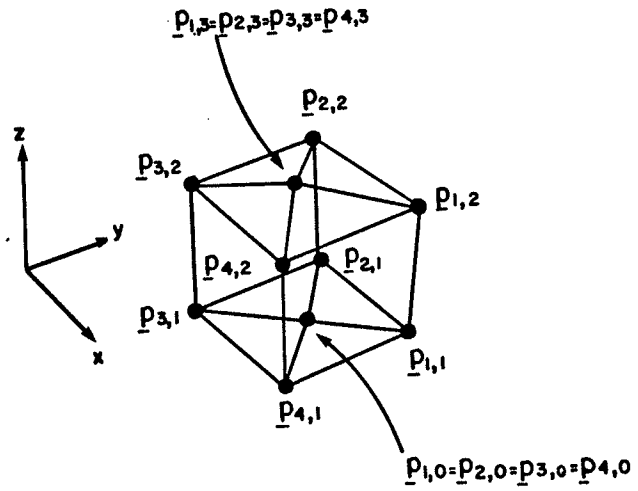

Figure 3.13: A closed network of ten points in R^3.

As an example, consider the closed network of ten points in R^3 (Figure 3.13). To interpolate this combination of points requires (m)(n)=12 bicubic surface patches (m=4, n=3) supported by (m+3)(n+3)=42 control vertices. The resulting (m)(n+1)=16 patch-corner equations are give as

$$\underline{P}_{i,j}^{(1,0)} = [\underline{V}_{i-1,j-2} + 4\underline{V}_{i,j-2} + \underline{V}_{i+1,j-2} + 4\underline{V}_{i-1,j-1} + 16\underline{V}_{i,j-1} + 4\underline{V}_{i+1,j-1} + \underline{V}_{i-1,j} + 4\underline{V}_{i,j} + \underline{V}_{i+1,j}]/36 = \underline{P}_{i,j-1} \qquad (3.100)$$

$$i = 1,2,\ldots,4 \quad j = 1,2,3 \ ,$$

and

$$\underline{P}_{i,j}^{(1,1)} = [\underline{V}_{i-1,j-1} + 4\underline{V}_{i,j-1} + \underline{V}_{i+1,j-1} + 4\underline{V}_{i-1,j} + 16\underline{V}_{i,j} + 4\underline{V}_{i+1,j} + \underline{V}_{i-1,j+1} + 4\underline{V}_{i,j+1} + \underline{V}_{i+1,j+1}]/36 = \underline{P}_{i,j} \qquad (3.101)$$

$$i = 1,2,\ldots,4 \quad j = 1,2,3 \ .$$

Expanding (3.100) and (3.101) yields

$$\underline{P}_{1,1}(1,0) = [\underline{V}_{0,-1} + 4\underline{V}_{1,-1} + \underline{V}_{2,-1} + 4\underline{V}_{0,0} + 16\underline{V}_{1,0} + 4\underline{V}_{2,0} + \underline{V}_{0,1} + 4\underline{V}_{1,1} + \underline{V}_{2,1}] = 36\underline{p}_{1,0}$$

$$\underline{P}_{1,1}(1,1) = [\underline{V}_{0,0} + 4\underline{V}_{1,0} + \underline{V}_{2,0} + 4\underline{V}_{0,1} + 16\underline{V}_{1,1} + 4\underline{V}_{2,1} + \underline{V}_{0,2} + 4\underline{V}_{1,2} + \underline{V}_{2,2}] = 36\underline{p}_{1,1}$$

$$\underline{P}_{1,2}(1,1) = [\underline{V}_{0,1} + 4\underline{V}_{1,1} + \underline{V}_{2,1} + 4\underline{V}_{0,2} + 16\underline{V}_{1,2} + 4\underline{V}_{2,2} + \underline{V}_{0,3} + 4\underline{V}_{1,3} + \underline{V}_{2,3}] = 36\underline{p}_{1,2}$$

$$\underline{P}_{1,3}(1,1) = [\underline{V}_{0,2} + 4\underline{V}_{1,2} + \underline{V}_{2,2} + 4\underline{V}_{0,3} + 16\underline{V}_{1,3} + 4\underline{V}_{2,3} + \underline{V}_{0,4} + 4\underline{V}_{1,4} + \underline{V}_{2,4}] = 36\underline{p}_{1,3}$$

$$\underline{P}_{2,1}(1,0) = [\underline{V}_{1,-1} + 4\underline{V}_{2,-1} + \underline{V}_{3,-1} + 4\underline{V}_{1,0} + 16\underline{V}_{2,0} + 4\underline{V}_{3,0} + \underline{V}_{1,1} + 4\underline{V}_{2,1} + \underline{V}_{3,1}] = 36\underline{p}_{2,0}$$

$$\underline{P}_{2,1}(1,1) = [\underline{V}_{1,0} + 4\underline{V}_{2,0} + \underline{V}_{3,0} + 4\underline{V}_{1,1} + 16\underline{V}_{2,1} + 4\underline{V}_{3,1} + \underline{V}_{1,2} + 4\underline{V}_{2,2} + \underline{V}_{3,2}] = 36\underline{p}_{2,1}$$

$$\underline{P}_{2,2}(1,1) = [\underline{V}_{1,1} + 4\underline{V}_{2,1} + \underline{V}_{3,1} + 4\underline{V}_{1,2} + 16\underline{V}_{2,2} + 4\underline{V}_{3,2} + \underline{V}_{1,3} + 4\underline{V}_{2,3} + \underline{V}_{3,3}] = 36\underline{p}_{2,2}$$

$$\underline{P}_{2,3}(1,1) = [\underline{V}_{1,2} + 4\underline{V}_{2,2} + \underline{V}_{3,2} + 4\underline{V}_{1,3} + 16\underline{V}_{2,3} + 4\underline{V}_{3,3} + \underline{V}_{1,4} + 4\underline{V}_{2,4} + \underline{V}_{3,4}] = 36\underline{p}_{2,3} \qquad (3.102)$$

$$\underline{P}_{3,1}(1,0) = [\underline{V}_{2,-1} + 4\underline{V}_{3,-1} + \underline{V}_{4,-1} + 4\underline{V}_{2,0} + 16\underline{V}_{3,0} + 4\underline{V}_{4,0} + \underline{V}_{2,1} + 4\underline{V}_{3,1} + \underline{V}_{4,1}] = 36\underline{p}_{3,0}$$

$$\underline{P}_{3,1}(1,1) = [\underline{V}_{2,0} + 4\underline{V}_{3,0} + \underline{V}_{4,0} + 4\underline{V}_{2,1} + 16\underline{V}_{3,1} + 4\underline{V}_{4,1} + \underline{V}_{2,2} + 4\underline{V}_{3,2} + \underline{V}_{4,2}] = 36\underline{p}_{3,1}$$

$$\underline{P}_{3,2}(1,1) = [\underline{V}_{2,1} + 4\underline{V}_{3,1} + \underline{V}_{4,1} + 4\underline{V}_{2,2} + 16\underline{V}_{3,2} + 4\underline{V}_{4,2} + \underline{V}_{2,3} + 4\underline{V}_{3,3} + \underline{V}_{4,3}] = 36\underline{p}_{3,2}$$

$$\underline{P}_{3,3}(1,1) = [\underline{V}_{2,2} + 4\underline{V}_{3,2} + \underline{V}_{4,2} + 4\underline{V}_{2,3} + 16\underline{V}_{3,3} + 4\underline{V}_{4,3} + \underline{V}_{2,4} + 4\underline{V}_{3,4} + \underline{V}_{4,4}] = 36\underline{p}_{3,3}$$

$$\underline{P}_{4,1}(1,0) = [\underline{V}_{3,-1} + 4\underline{V}_{4,-1} + \underline{V}_{5,-1} + 4\underline{V}_{3,0} + 16\underline{V}_{4,0} + 4\underline{V}_{5,0} + \underline{V}_{3,1} + 4\underline{V}_{4,1} + \underline{V}_{5,1}] = 36\underline{p}_{4,0}$$

$$\underline{P}_{4,1}(1,1) = [\underline{V}_{3,0} + 4\underline{V}_{4,0} + \underline{V}_{5,0} + 4\underline{V}_{3,1} + 16\underline{V}_{4,1} + 4\underline{V}_{5,1} + \underline{V}_{3,2} + 4\underline{V}_{4,2} + \underline{V}_{5,2}] = 36\underline{p}_{4,1}$$

$$\underline{P}_{4,2}(1,1) = [\underline{V}_{3,1} + 4\underline{V}_{4,1} + \underline{V}_{5,1} + 4\underline{V}_{3,2} + 16\underline{V}_{4,2} + 4\underline{V}_{5,2} + \underline{V}_{3,3} + 4\underline{V}_{4,3} + \underline{V}_{5,3}] = 36\underline{p}_{4,2}$$

$$\underline{P}_{4,3}(1,1) = [\underline{V}_{3,2} + 4\underline{V}_{4,2} + \underline{V}_{5,2} + 4\underline{V}_{3,3} + 16\underline{V}_{4,3} + 4\underline{V}_{5,3} + \underline{V}_{3,4} + 4\underline{V}_{4,4} + \underline{V}_{5,4}] = 36\underline{p}_{4,3}$$

The control vertex constraints can be explicitly written as

$$\begin{aligned} \underline{V}_{0,j} &= \underline{V}_{4,j} \\ \underline{V}_{-1,j} &= \underline{V}_{3,j} \qquad j = -1,0,1,\ldots,4 \ , \\ \underline{V}_{5,j} &= \underline{V}_{1,j} \end{aligned} \tag{3.103}$$

and

$$\begin{aligned} \underline{V}_{i,4} &= \underline{V}_{k,2} \\ \underline{V}_{i,-1} &= \underline{V}_{k,1} \end{aligned} \qquad i = 1,2,\ldots,4 \qquad k = \begin{cases} i + 2 & i \leq 2 \\ i - 2 & i > 2 \end{cases} . \tag{3.104}$$

Applying the above constraints to the sixteen patch-corner

equations yields

$$\underline{P}_{1,1}(1,0) = [\underline{V}_{2,1} + 4\underline{V}_{3,1} + \underline{V}_{4,1} + 4\underline{V}_{4,0} + 16\underline{V}_{1,0} + 4\underline{V}_{2,0} + \underline{V}_{4,1} + 4\underline{V}_{1,1} + \underline{V}_{2,1}] = 36\underline{p}_{1,0}$$

$$\underline{P}_{1,1}(1,1) = [\underline{V}_{4,0} + 4\underline{V}_{1,0} + \underline{V}_{2,0} + 4\underline{V}_{4,1} + 16\underline{V}_{1,1} + 4\underline{V}_{2,1} + \underline{V}_{4,2} + 4\underline{V}_{1,2} + \underline{V}_{2,2}] = 36\underline{p}_{1,1}$$

$$\underline{P}_{1,2}(1,1) = [\underline{V}_{4,1} + 4\underline{V}_{1,1} + \underline{V}_{2,1} + 4\underline{V}_{4,2} + 16\underline{V}_{1,2} + 4\underline{V}_{2,2} + \underline{V}_{4,2} + 4\underline{V}_{1,3} + \underline{V}_{2,3}] = 36\underline{p}_{1,2}$$

$$\underline{P}_{1,3}(1,1) = [\underline{V}_{4,2} + 4\underline{V}_{1,2} + \underline{V}_{2,2} + 4\underline{V}_{4,3} + 16\underline{V}_{1,3} + 4\underline{V}_{2,3} + \underline{V}_{2,2} + 4\underline{V}_{3,2} + \underline{V}_{4,2}] = 36\underline{p}_{1,3}$$

$$\underline{P}_{2,1}(1,0) = [\underline{V}_{3,1} + 4\underline{V}_{4,1} + \underline{V}_{1,1} + 4\underline{V}_{1,0} + 16\underline{V}_{2,0} + 4\underline{V}_{3,0} + \underline{V}_{1,1} + 4\underline{V}_{2,1} + \underline{V}_{3,1}] = 36\underline{p}_{2,0}$$

$$\underline{P}_{2,1}(1,1) = [\underline{V}_{1,0} + 4\underline{V}_{2,0} + \underline{V}_{3,0} + 4\underline{V}_{1,1} + 16\underline{V}_{2,1} + 4\underline{V}_{3,1} + \underline{V}_{1,2} + 4\underline{V}_{2,2} + \underline{V}_{3,2}] = 36\underline{p}_{2,1}$$

$$\underline{P}_{2,2}(1,1) = [\underline{V}_{1,1} + 4\underline{V}_{2,1} + \underline{V}_{3,1} + 4\underline{V}_{1,2} + 16\underline{V}_{2,2} + 4\underline{V}_{3,2} + \underline{V}_{1,3} + 4\underline{V}_{2,3} + \underline{V}_{3,3}] = 36\underline{p}_{2,2}$$

$$\underline{P}_{2,3}(1,1) = [\underline{V}_{1,2} + 4\underline{V}_{2,2} + \underline{V}_{3,2} + 4\underline{V}_{1,3} + 16\underline{V}_{2,3} + 4\underline{V}_{3,3} + \underline{V}_{3,2} + 4\underline{V}_{4,2} + \underline{V}_{1,2}] = 36\underline{p}_{2,3} \qquad (3.105)$$

$$\underline{P}_{3,1}(1,0) = [\underline{V}_{4,1} + 4\underline{V}_{1,1} + \underline{V}_{2,1} + 4\underline{V}_{2,0} + 16\underline{V}_{3,0} + 4\underline{V}_{4,0} + \underline{V}_{2,1} + 4\underline{V}_{3,1} + \underline{V}_{4,1}] = 36\underline{p}_{3,0}$$

$$\underline{P}_{3,1}(1,1) = [\underline{V}_{2,0} + 4\underline{V}_{3,0} + \underline{V}_{4,0} + 4\underline{V}_{2,1} + 16\underline{V}_{3,1} + 4\underline{V}_{4,1} + \underline{V}_{2,2} + 4\underline{V}_{3,2} + \underline{V}_{4,2}] = 36\underline{p}_{3,1}$$

$$\underline{P}_{3,2}(1,1) = [\underline{V}_{2,1} + 4\underline{V}_{3,1} + \underline{V}_{4,1} + 4\underline{V}_{2,2} + 16\underline{V}_{3,2} + 4\underline{V}_{4,2} + \underline{V}_{2,3} + 4\underline{V}_{3,3} + \underline{V}_{4,3}] = 36\underline{p}_{3,2}$$

$$\underline{P}_{3,3}(1,1) = [\underline{V}_{2,2} + 4\underline{V}_{3,2} + \underline{V}_{4,2} + 4\underline{V}_{2,3} + 16\underline{V}_{3,3} + 4\underline{V}_{4,3} + \underline{V}_{4,2} + 4\underline{V}_{1,2} + \underline{V}_{2,2}] = 36\underline{p}_{3,3}$$

$$\underline{P}_{4,1}(1,0) = [\underline{V}_{1,1} + 4\underline{V}_{2,1} + \underline{V}_{3,1} + 4\underline{V}_{3,0} + 16\underline{V}_{4,0} + 4\underline{V}_{1,0} + \underline{V}_{3,1} + 4\underline{V}_{4,1} + \underline{V}_{1,1}] = 36\underline{p}_{4,0}$$

$$\underline{P}_{4,1}(1,1) = [\underline{V}_{3,0} + 4\underline{V}_{4,0} + \underline{V}_{1,0} + 4\underline{V}_{3,1} + 16\underline{V}_{4,1} + 4\underline{V}_{1,1} + \underline{V}_{3,2} + 4\underline{V}_{4,2} + \underline{V}_{1,2}] = 36\underline{p}_{4,1}$$

$$\underline{P}_{4,2}(1,1) = [\underline{V}_{3,1} + 4\underline{V}_{4,1} + \underline{V}_{1,1} + 4\underline{V}_{3,2} + 16\underline{V}_{4,2} + 4\underline{V}_{1,2} + \underline{V}_{3,3} + 4\underline{V}_{4,3} + \underline{V}_{1,3}] = 36\underline{p}_{4,2}$$

$$\underline{P}_{4,3}(1,1) = [\underline{V}_{3,2} + 4\underline{V}_{4,2} + \underline{V}_{1,2} + 4\underline{V}_{3,3} + 16\underline{V}_{4,3} + 4\underline{V}_{1,3} + \underline{V}_{1,2} + 4\underline{V}_{2,2} + \underline{V}_{3,2}] = 36\underline{p}_{4,3}$$

Thus, the system is reduced to (m)(n+1) equations in (m)(n+1) distinct control vertices:

$$\underline{V}_{i,j} \quad i = 1,2,\ldots,4 \quad j = 0,1,\ldots,3 \; . \tag{3.106}$$

In matrix notation, (3.105) can be represented as

$$[C][\underline{V}] = [\underline{p}] \; . \tag{3.107}$$

where

$$[\underline{V}] = \begin{bmatrix} \underline{V}_{1,0} \\ \underline{V}_{1,1} \\ \underline{V}_{1,2} \\ \underline{V}_{1,3} \\ \underline{V}_{2,0} \\ \underline{V}_{2,1} \\ \underline{V}_{2,2} \\ \underline{V}_{2,3} \\ \underline{V}_{3,0} \\ \underline{V}_{3,1} \\ \underline{V}_{3,2} \\ \underline{V}_{3,3} \\ \underline{V}_{4,0} \\ \underline{V}_{4,1} \\ \underline{V}_{4,2} \\ \underline{V}_{4,3} \end{bmatrix} \; , \quad [C] = \begin{bmatrix} 1 & 6 & 4 & & & 4 & 2 & & & & 4 & & & 4 & 2 & & \\ & 4 & 16 & 4 & & 1 & 4 & 1 & & & & & & 1 & 4 & 1 & \\ & & 4 & 16 & 4 & & 1 & 4 & 1 & & & & & & 1 & 4 & 1 \\ & & & 4 & 16 & & & 2 & 4 & & & 4 & & & & 2 & 4 \\ & 4 & 2 & & & 16 & 4 & & & 4 & 2 & & & & 4 & & \\ & 1 & 4 & 1 & & 4 & 16 & 4 & & 1 & 4 & 1 & & & & & \\ & & 1 & 4 & 1 & & 4 & 16 & 4 & & 1 & 4 & 1 & & & & \\ & & & 2 & 4 & & & 4 & 16 & & & 2 & 4 & & & 4 & \\ & & 4 & & & 4 & 2 & & & 16 & 4 & & & 4 & 2 & & \\ & & & & & 1 & 4 & 1 & & 4 & 16 & 4 & & 1 & 4 & 1 & \\ & & & & & & 1 & 4 & 1 & & 4 & 16 & 4 & & 1 & 4 & 1 \\ & & & 4 & & & & 2 & 4 & & & 4 & 16 & & & 2 & 4 \\ & 4 & 2 & & & & 4 & & & 4 & 2 & & & 16 & 4 & & \\ & 1 & 4 & 1 & & & & & & 1 & 4 & 1 & & 4 & 16 & 4 & \\ & & 1 & 4 & 1 & & & & & & 1 & 4 & 1 & & 4 & 16 & 4 \\ & & & 2 & 4 & & & 4 & & & & 2 & 4 & & & 4 & 16 \end{bmatrix} \; , \quad [p] = 36^{*} \begin{bmatrix} \underline{p}_{1,0} \\ \underline{p}_{1,1} \\ \underline{p}_{1,2} \\ \underline{p}_{1,3} \\ \underline{p}_{2,0} \\ \underline{p}_{2,1} \\ \underline{p}_{2,2} \\ \underline{p}_{2,3} \\ \underline{p}_{3,0} \\ \underline{p}_{3,1} \\ \underline{p}_{3,2} \\ \underline{p}_{3,3} \\ \underline{p}_{4,0} \\ \underline{p}_{4,1} \\ \underline{p}_{4,2} \\ \underline{p}_{4,3} \end{bmatrix} \; . \tag{3.108}$$

For the closed network of points in Figure 3.13, the $\underline{p}$

vector in (3.108) possesses the characteristic

$$\underline{P}_{1,0} = \underline{P}_{2,0} = \underline{P}_{3,0} = \underline{P}_{4,0} \,, \qquad \underline{P}_{1,3} = \underline{P}_{2,3} = \underline{P}_{3,3} = \underline{P}_{4,3} \,. \tag{3.109}$$

If the network of points is altered to a quasi-closed formation, only the $\underline{p}$ vector needs to be modified. The C-matrix is completely transparent to the point configuration. As a result, for a particular m by n surface patch combination, any arrangement of (m)(n+1) points can be interpolated without reconstructing the coefficient matrix.

3.2.5 Solution Technique Considerations

The coefficient matrix generated by the closed and quasi-closed surface formulations is nonsymmetric and sparse. The number of nonzero entries in relation to the zero entries can be expressed as

$$\frac{9(m)(n+1)}{[(m)(n+1)]^2 - 9(m)(n+1)} = \frac{9}{(m)(n+1) - 9} \quad (m = 6,8,10,\ldots) \quad (n = 3,4,5,\ldots) \,. \tag{3.110}$$

As the number of points to be interpolated grows, the C-matrix becomes increasingly filled with zero entries. In order to avoid the unnecessary storage of zeros, a solution technique that incorporates a sparse storage scheme is essential.

The C-matrix also possesses the characteristic of diagonal dominance with no zero entries located on the diagonal. As a consequence, solution techniques which utilize diagonal pivoting can be implemented.

The major factor in determining the control vertices and hence, generating a surface, lies in the fact that the $\underline{V}$ and $\underline{p}$ vectors have entries with x, y, and z components.

$$\underline{V}_{i,j} = [Vx_{i,j}\ Vy_{i,j}\ Vz_{i,j}] \quad \underline{p}_{i,j} = [x_{i,j}\ y_{i,j}\ z_{i,j}] \ . \qquad (3.111)$$

Thus, to obtain the complete $\underline{V}$ vector representation the following is implemented:

$$\begin{aligned} [Vx] &= [C]^{-1}[x] \ , \\ [Vy] &= [C]^{-1}[y] \ , \\ [Vz] &= [C]^{-1}[z] \ . \end{aligned} \qquad (3.112)$$

Since the inverse of the coefficient matrix needs to be multiplied by each component of the $\underline{p}$ vector, a direct method incorporating the product form of the inverse is desirable. This is especially so where real-time execution of the algorithm is needed.

A modified bi-factorization technique (after Zollenkopf [9]) incorporates all of the above considerations. The

C-matrix is stored using a double linked-list scheme which avoids the unnecessary storage of zero entries. The inverse is obtained by factoring the coefficient matrix into several factor matrices. This product form of the inverse is then multiplied by each component of the $\underline{p}$ vector to obtain the coordinates of the distinct control vertices.

Chapter IV

CLOSED AND QUASI-CLOSED IMPLEMENTATIONS

The theory developed in the preceding sections has been implemented in a interactive surface modelling package. The package consists of two phases:

1. data preparation and
2. surface interpolation.

The first phase in the modelling process is to specify the network of points to be interpolated. The point network is prescribed by interactive menu selections and can be manipulated into a closed or quasi-closed form. The second phase generates the system coefficient matrix and determines the corresponding control vertices based upon the problem dimension (m and n). The control vertices are used in conjunction with the uniform bicubic basis to generate a closed or quasi-closed interpolating surface.

The surface display implementation makes extensive use of windowed menu selection as a means of user interaction. Menu features include the ability to observe the surface from various viewpoints. In addition, increased patch definition is provided by the subdivision feature which partitions individual patches with constant-parameter lines. This is particularly useful in regions of higher curvature,

where more definition is required to discern the surface shape.

The surfaces generated by the closed and quasi-closed algorithms are solid. The manner by which the surfaces are displayed can be conceptualized as transparent shells with inked lines drawn about to exemplify shape. This inked line representation can be misleading since individual lines can fluctuate perpendicular to the surface normal, giving the appearance of surface undulations. If one were to implement such algorithms on a graphics device capable of shading, the surface representation would appear as a smooth continuous shell.

In order to demonstrate the functional aspects of the closed and quasi-closed modelling schemes, a number of examples are provided in the following sections.

4.1 A CLOSED BICUBIC SURFACE

Recall that in the closed surface formulation the control vertex structure, combined with the patch-corner point constraints (at the v-parameter extremes), interpolates a closed network of points.

Consider interpolating a network of (m)(n+1)=24 points in R^3. This translates to (m)(n-1)+2=14 distinct points in the closed formulation (See (3.20)). This underlying network is illustrated in Figure 4.1. The corresponding surface patch arrangement (Figure 4.2) clearly interpolates the closed

network. In particular, the surface appears well behaved at the v-parameter extremes.

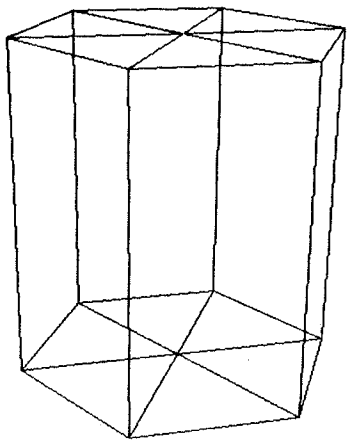

Figure 4.1: A closed network of 24 distinct points (m=6,n=3).

To demonstrate the localized influence of the surface in Figure 4.2, consider altering a single point in the closed network (Figure 4.3). The resulting surface (Figure 4.4) illustrates that the effect of the perturbation is sensed locally.

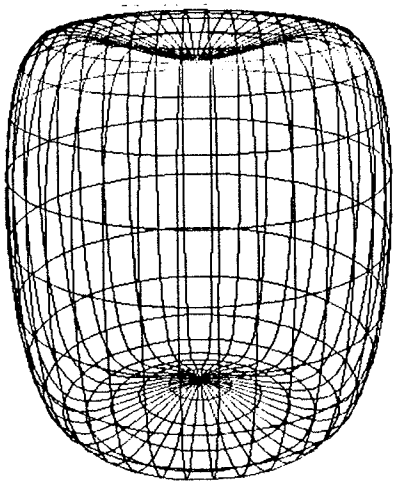

Figure 4.2: Closed interpolating surface (m=6,n=3).

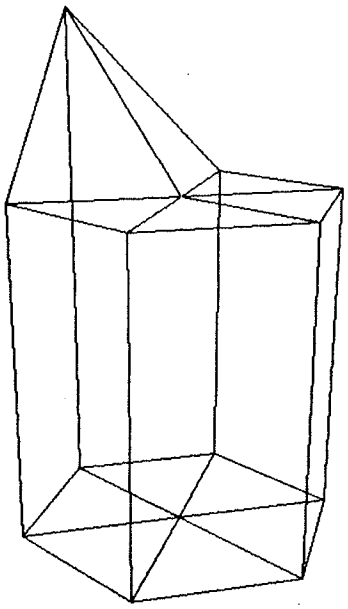

Figure 4.3: A closed network with a point perturbation.

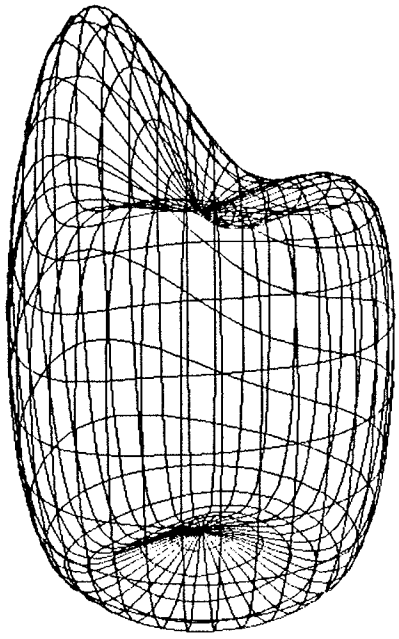

Figure 4.4: Localized effects of a point perturbation.

4.2 A QUASI-CLOSED SURFACE OPENED AT ONE EXTREME.

The quest for realistic graphic object representation in analytic and synthetic applications has recently been an area of widespread interest.

In many analytic applications, designers of three-dimensional objects would like to preview preliminary designs and subject them to various computer simulated analyses. In this regard, the closed bicubic B-spline formulation is a useful and practical design tool. It provides positional, first derivative, and second derivative continuity, and, as a result, inherently ensures the continuity of surface normal components. Moreover, surface

normal calculations are easily determined. This is of particular importance for geometric modelling in such advanced numerical techniques as the Boundary Element Method [21, 22].

Conventionally, for most synthetic applications, achieving a viable object representation meant interconnecting immense numbers of polygons. In order to process such information, the polygon description must be organized into an enormous data base consisting of vertices, edges and polygons. On the other hand, the closed bicubic B-spline formulation allows for complex surface definition with a minimal amount of effort. All that need be supplied are the points for interpolation.

For example, consider the quasi-closed surface illustrated in Figure 4.5. The surface is comprised of m=20 by n=18 bicubic patches, interpolating (m)(n+1)=380 points arranged in a quasi-closed formation. To achieve a comparable surface structure implementing a polygon representation would require at least 1440 polygons and 1460 points. By comparison, the quasi-closed surface can be completely defined by the (m)(n+1)=380 distinct control vertices which support the surface. This has obvious advantages in terms of storage requirements. Moreover , surface rotations require that only the control vertices be transformed, which is advantageous for real-time execution.

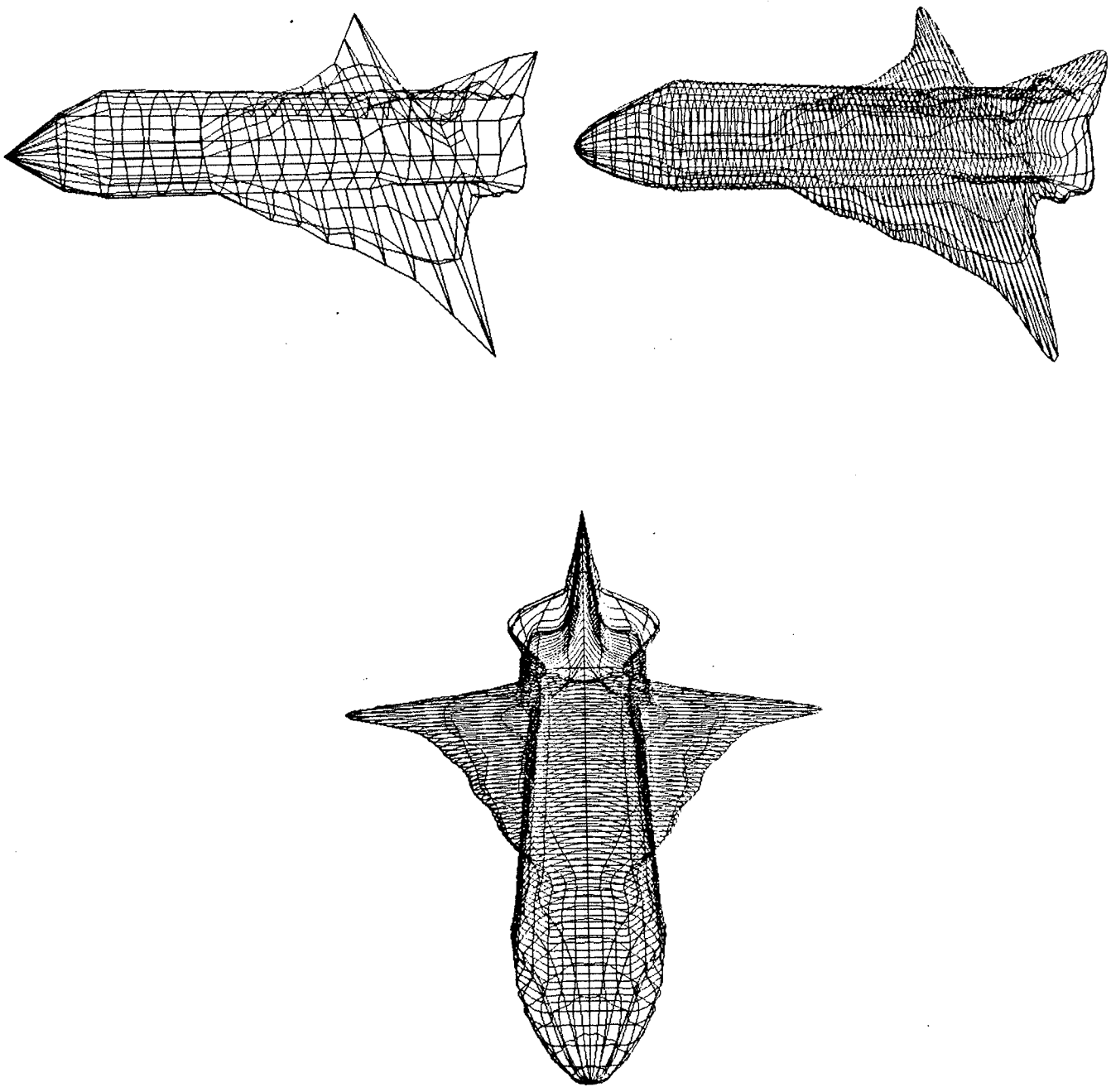

Figure 4.5: A quasi-closed surface opened at one extreme.

4.3 QUASI-CLOSED SURFACE OPENED AT BOTH EXTREMES

To form quasi-closed surfaces opened at both extremes the patch corner point constraints can be removed from the formulation. This allows the surface to interpolate (m)(n+1) distinct points.

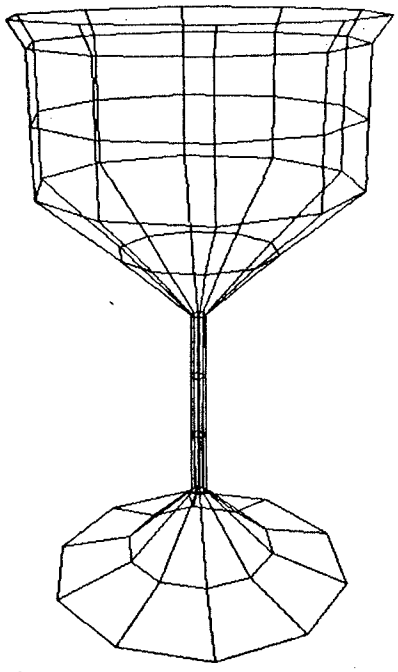

Figure 4.6: A quasi-closed network of point opened at both v extremes.

Consider the quasi-closed network of (m)(n+1)=110 points in Figure 4.6. Clearly the surface is opened at both v-parameter extremes. If the network of points is interpolated with bicubic B-spline surface patches, there is evidence of the surface-edge artifact (Figure 4.7). Recall that this occurs because of the underlying control vertex structure. By adding constant-parameter lines within each patch, the surface definition becomes more detailed.

Moreover, the surface-edge undulations seem to add to the surface representation rather than detract (Figure 4.8).

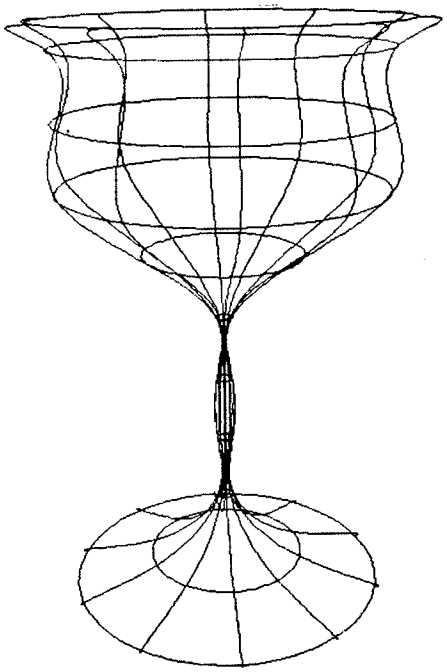

Figure 4.7: Quasi-closed surface with surface-edge artifacts.

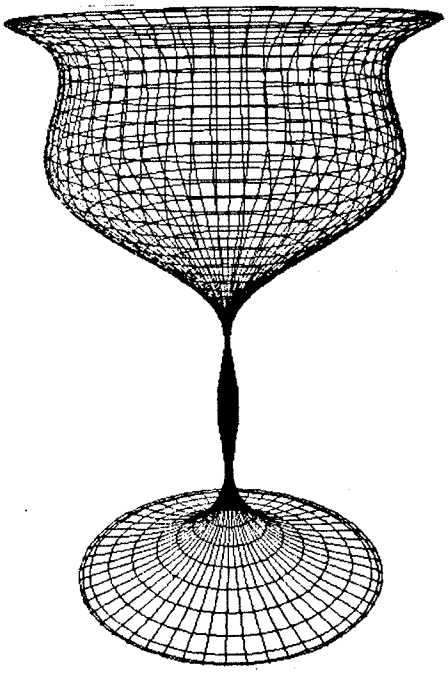

Figure 4.8: Surface highlighted with constant-parameter lines.

4.4 MULTI-OBJECT REPRESENTATION

For many applications it is necessary to display a collection of surfaces. This is particularly useful in medical applications where the visual representation of internal body organs and their positions with respect to each other is an important diagnostic tool.

The closed bicubic B-spline formulation shows promise as a modelling scheme for such applications. Since many components of the human anatomy are comprised of smooth continuous surfaces, the closed and quasi-closed representations[2] can adequately portray such structures (Figure 4.9).

The present algorithm does not cater to the simultaneous manipulation of more than one surface. However, a multi-object environment can be simulated by concurrently displaying any number of surfaces without refreshing the display device. To alter a viewpoint, each surface be individually processed then displayed.

---

[2] The surfaces are depicted by a reduced set of points to alleviate misleading fluctuations in the representation.

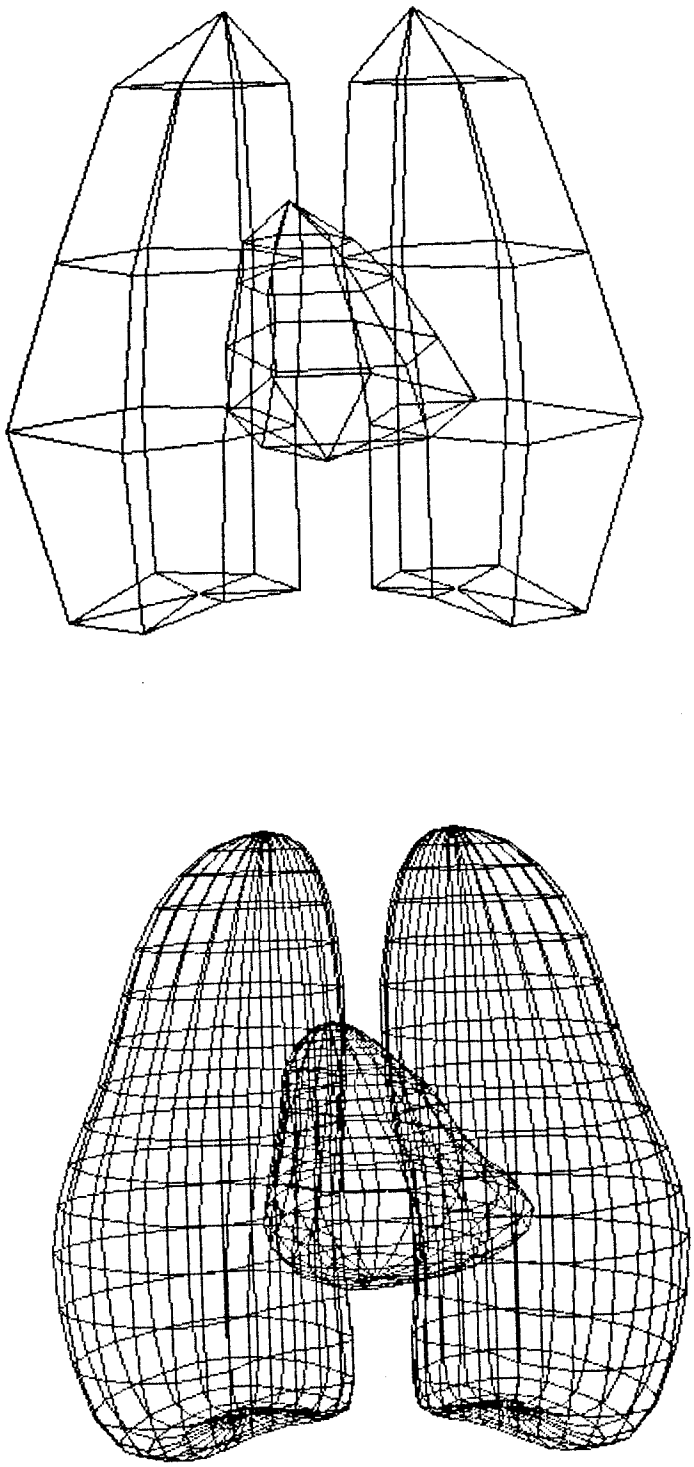

Figure 4.9: A multi-object representation of the heart and lungs.

Chapter V

CONCLUSIONS

Recent work by Barsky [6, 7, 13, 15] addresses the formulation of bicubic B-spline surfaces for interpolating open point networks. In this thesis, a novel approach to modelling closed and quasi-closed surfaces through the use of a closed uniform bicubic B-spline formulation has been presented. The formulation is derived to interpolate a closed network of points in R^3. The surface closure is attained by transforming both the surface patch arrangement and the controlling vertex structure to a specified closed form. This is accomplished by the introduction of patch-corner point contraints and control vertex constraints.

The closed control vertex structure plays a significant part in assuring a closed surface formulation. Firstly, positional, first derivative, and second derivative continuity is inherently guaranteed everywhere on the surface, thus alleviating the necessity of specifying derivative boundary constraints along the patch merger. Secondly, the transformation to the closed control vertex structure introduces the appropriate number of constraints to yield a completely determinable system of equations.

The closed surface formulation is extended to include quasi-closed surfaces by disregarding certain patch-corner point constraints. As a result, this extension to quasi-closed surfaces does not introduce additional system equations. Only the network of points on the surface is modified. Thus, for a particular number of surface patches, the coefficient matrices generated by the closed and quasi-closed formulations are indistinguishable.

The quasi-closed formulation generates surface-edge artifacts about the v extremes when the combined constraints of interpolation and control-structure influence are overwhelming. This possibly can be circumvented by introducing additional interpolation points.

The closed bicubic B-spline formulation demonstrates merit as a geometric modelling scheme for both analytic and synthetic applications. The inherent results of positional, first derivative, and second derivative surface continuity is advantages in computational methods which rely upon accurate object representation.

In synthetic applications, the closed surface formulation allows for complex surface definition with a minimum of effort. Object representation requires less storage and computational effort than similar polygon structures.

The formulation falls short of depicting closed surfaces containing edge discontinuities. To implement edges in a bicubic B-spline surface, cusps must be introduced by way of

multiple control vertices [12]. This, along with a unified approach to modelling a multiple object environment implementing hidden and shaded surface techniques, would greatly enhance the geometric flexibility of the method.

REFERENCES

1. Coons, S. A., 'Surfaces for Computer Aided Design of Space Forms', MIT Project MAC TR-41, June 1964.

2. Ferguson, J. C., 'Multivariable Curve Interpolation,' J. ACM, Vol. 2 (April 1964), pp. 221-228.

3. Peters, G. J., 'Interactive Computer Graphics Application of the Parametric Bicubic Surface to Engineering Design Problems,' in Computer Aided Geometric Design, (ed. R. E. Barnhill and R. F. Riesenfeld), Academic Press, New York, 1974, p. 279.

4. Barnhill, R. E., Brown, J. H., and I. M. Klucewicz, 'A New Twist in Computer Aided Design,' Comput. Graph. Image Proc., Vol.8 No.1, (August 1978) p. 78.

5. Coons, S. A., 'Surface Patches and B-Spline Curves,' in Computer Aided Geometric Design, (ed. R. E. Barnhill and R. F. Riesenfeld), Academic Press, New York, 1974, p. 6.

6. Barsky, B. A., and D.P. Greenberg, 'Determining a Set of B-Spline Control Vertices to Generate an Interpolating Surface,' Comput. Graph. Image Proc., Vol. 14 No. 3 (November 1980), pp.203-226.

7. Barsky, B. A., and D. P. Greenberg, 'Interactive Surface Representation System using a B-Spline Formulation with Interpolation Capability', Comput. Aided. Des., Vol. 14 No. 4 (July 1982), pp 187-194.

8. Catmull, E. and J. Clark, 'Recursively Generated B-Spline Surfaces on Arbitrary Topological Meshes,' Comput. Aided Des., Vol. 10 No. 6 (November 1978), pp.350-355.

9. Zollenkopf, K., 'Bi-Factorization - Basic Computational Algorithm and Programming Techniques', in Sparse Matrices and their Applications, (ed. J. K. Reid), Plenum Press, New York and London, 1972, pp.75-96.

10. Forrest, A. R., 'Interactive Interpolation and Approximation by Bezier Polynomial', Comput. J., Vol. 15 (1972), pp.71-79.

11. Gordon, W. J. and R. F. Riesenfeld, 'Bernstein-Bezier Methods for the Computer Aided Design of Free Form Curves and Surfaces', J. ACM., Vol. 21, No. 2 (April 1974), pp.293-310.

12. Gordon, W. J., and R. F. Riesenfeld, 'B-spline Curves and Surfaces', in Computer Aided Geometric Design, (ed. R. E. Barnhill and R. F. Riesenfeld), Academic Press, New York, 1974, pp. 110-113.

13. Barsky, B. A., and J. C. Beatty, 'Local Control of Bias and Tension in Beta-splines', ACM Trans. Graph., Vol. 2, No. 2 (April 1983), pp.109-134.

14. Pilcher, D.,'Smooth Parametric Surfaces', in Computer Aided Geometric Design, (ed. R. E. Barnhill and R. F. Riesenfeld), Academic Press, New York, 1974, pp. 237-253.

15. Barsky, B. A., 'End Conditions and Boundary Conditions for Uniform B-spline Curve and Surface Representation', Comput. Ind., Vol. 3, Nos. 1, 2, (March, June 1982), pp. 17-29.

16. Overhauser, A. W., 'Analytic Definition of Curves and Surfaces by Parabolic Blending', Technical Report SL68-40, Scientific Research Staff Publications, Ford Motor Company, 1968.

17. Brewer, J. A., and D. C. Anderson, 'Visual Interaction with Overhauser Curves and Surfaces', Proc. SIGGRAPH (July 1977), pp.132-137.

18. Wu, S., and J. F. Abel, 'Representation and Discretization of Arbitrary Surfaces for Finite Element Shell Analysis', Inter. J. Numer. Meth., Vol. 14, 1979, pp. 813-836.

19. Wu, S., J. F. Abel and D. P. Greenberg, 'An Interactive Computer Graphics Approach to Surface Representation', Graph. Image Process., Vol. 20, No. 10 (October 1977), pp.703-712.

20. Prenter, P. M., Splines and Variational Methods, John Wiley & Sons, New York, 1975, p. 135.

21. Bilgen, S., Cubic Spline Elements for Boundary Integral Equations, Ph.D. Dissertation, University of Manitoba, 1982.

22. Lean, M. H., Electromagnetic Field Solution with the Boundary Element Method, Ph.D. Dissertation, University of Manitoba, 1981.